DRAFT

Performance of Drained and Undrained Flexible Pavement Structures under Wet Conditions

Accelerated Test Data

Test Section 545–Undrained

Prepared for:

California Department of Transportation

by:

Manuel O. Bejarano, John T. Harvey, Abdikarim Ali,
David Mahama, Dave Hung, and Pitipat Preedonant

December 2001
Revision 2004

Pavement Research Center
Institute of Transportation Studies
University of California at Berkeley

TABLE OF CONTENTS

LIST OF FIGURES

LIST OF TABLES

EXECUTIVE SUMMARY

This report is the third in a series that describes the results of accelerated pavement testing conducted on full-scale pavements at the Richmond Field Station (RFS). The report contains a summary of the results and associated analyses of a pavement section composed of three lifts of asphalt concrete and an untreated aggregate base layer on top of a prepared subgrade. The pavement section is termed an undrained pavement because it does not include an ATPB layer between the asphalt concrete layers and the untreated aggregate base. The pavement structure was designated Section 545. The tests on this test section have been performed as part of the Goal 5 Accelerated Test Program for the evaluation of drained and undrained pavements under conditions of water infiltration.

The main objective of the test program is:

- To develop data to quantitatively compare and evaluate the performance of reduced thickness asphalt rubber hot mix (ARHM) and full thickness of dense graded asphalt concrete (DGAC) mix on wearing courses for pavement structures with wet base conditions.

Other objectives are:

- To quantify elastic moduli of the pavement layers;
- To quantify the stress dependence of the pavement layers;
- To determine the mechanics of failure of the pavement structure;
- To evaluate the effectiveness of non-destructive and partially destructive methods for assessing pavement structural condition.

HVS testing was begun in April 2001 and was completed in August 2001 after the application of more than 742,000 load repetitions. At the end of the test, the pavement section had 9 mm of surface rutting and a surface crack density of 2.4 m of cracks per square meter.

Chapter 2 describes the test program for Section 545. Design and as-constructed thicknesses for the pavement components were as follows:

Layer	Design Thickness	As-Built Thickness
Dense graded asphalt concrete wearing course	75 mm	90 mm
Dense graded asphalt concrete	148 mm	143 mm
Aggregate base	182 mm	259 mm
Aggregate subbase	215 mm	206-280 mm

The test program was conducted in four stages. Stage 1 was intended to establish the initial structural condition of the section under conditions of no water infiltration. Stage 2 was intended to establish the initial structural condition of the section under water infiltration. Stage 3 was HVS trafficking under conditions of water infiltration. Stage 4 was intended to establish the structural condition of the section after HVS trafficking.

Data collection for Stages 1, 2, and 4 were based on the deflections obtained from the falling weight deflectometer (FWD) deflections and moisture content measurements. Stage 4 included some destructive and partially-destructive tests to verify results obtained during Stage 3.

Data collection for Stage 3 followed a schedule of the number of HVS load repetitions and the appearance of any pavement deterioration. Loading was applied by dual radial tires inflated to a pressure of 720 kPa and consisted of the following:

Load	Number of Repetitions
40 kN	147,000
80 kN	117,600
100 kN	477,310

Lateral wander of the wheels was over the one-meter width of the test section.

At the termination of loading, surface rutting and fatigue cracking were visible throughout the test section.

Measures of pavement responses were obtained with Multi-Depth Deflectometers (MDDs), the Road Surface Deflectometer (RSD), and the laser profilometer. Fatigue cracking was monitored using digital photography and a digital image analysis procedure. Thermocouples were used to measure air and pavement temperatures at various depths in the asphalt concrete. To maintain a constant temperature of approximately 20ºC, a temperature control cabinet was utilized. Chapter 3 summarizes the data obtained during the course of loading and associated analyses.

Rutting data indicates that Section 545 performed slightly better than Section 544. Differences seem to be due to performance of the asphalt concrete and aggregate base layers. Air-void content data indicated a significant reduction in the air-void content (increase in density) of the ARHM layer in Section 544. In contrast, no significant reduction in air-void content was observed for the DGAC layer in Section 545. Moduli of the AC layers were higher for Section 545 (6,000 to 10,000 MPa) than for Section 544 (5,000 to 7,500 MPa). Moduli of the aggregate base were lower for Section 545 than for Section 544.

1.0 INTRODUCTION

This report presents the data for the accelerated pavement testing (APT) program conducted on Heavy Vehicle Simulator (HVS) test Section 545. This section is part of the accelerated test program described in the test plan for CAL/APT Goal 5, "Performance of Drained and Undrained Flexible Pavement Structures under Wet Conditions."(*1*) Reference (*1*) provides detailed information on the Goal 5 APT program.

Section 545 (like Section 544) was tested to evaluate the performance of a typical California "undrained" pavement section under wet conditions and to compare its performance with that of Section 543 (a "drained" pavement section) in the same condition. Caltrans defines an "undrained" pavement section as a conventional flexible pavement that does not have a permeable layer between the asphalt concrete and the aggregate base. This, as noted in References (*1, 2*) contrasts with a "drained" pavement section, which is a conventional flexible pavement that includes a 75-mm layer of asphalt treated permeable base (ATPB) between the asphalt concrete and aggregate base connected to a drainage system at the shoulder. Reference (*1*) describes the purpose of the ATPB layer.

Wet conditions for Section 545 were intended to simulate approximate surface infiltration rates that would occur along the north coast climate region of California (*2*) during a wet month for a badly cracked asphalt concrete layer. Because the surface course of Section 545 was initially uncracked, water was introduced through small holes drilled through the asphalt concrete and into the aggregate base.

1.1 Objectives

The main objective of this test program was to measure and compare the long-term performance of undrained structures with ARHM-GG and DGAC wearing courses under wet

conditions. Other objectives included the following:

- Determine the failure mechanism of the pavement section;
- Quantify elastic moduli of the various pavement layers using deflections obtained from a slow moving wheel and from the falling weight deflectometer (FWD);
- Evaluate the effectiveness of non-destructive and partially destructive methods for assessing the pavement structural condition; these methods included:
  - Ground Penetrating Radar (GPR) and nuclear hydroprobes to measure water content, and
  - FWD to estimate moduli of the pavement layers.

This report, together with similar reports for each of the other two test sections (543 and 544), an earlier published laboratory report (*1*), special associated reports, and a summary report comprise the documentation of the results for the Goal 5 program.

The sequence of HVS testing of the three Goal 5 test sections was: 1) Section 543 (drained), 2) Section 544 (undrained), and 3) Section 545 (undrained).

1.2 Organization of Report

Chapter 2 contains a description of the test program for Section 545, including loading sequence, instrumentation , and data collection scheme. Chapter 3 presents a summary and analysis of the data collected during the test. Analyses include back-calculated moduli from deflection tests and their effectiveness to establish structural condition. Chapter 4 presents mechanistic analyses of Section 545 to evaluate the performance and compare its performance to that of the other undrained section (Section 544). Chapter 5 contains a summary of the results and conclusions.

2.0 TEST PROGRAM

This section describes the test section layout, environmental conditions encountered during the test, instrumentation used to collect data, and the test program.

2.1 Test Section Layout

Section 545 is 8 m long by 1 m wide. This area was divided into sixteen 0.5-m long by 1.0-m wide segments distinguished by stations numbered 0 to 16, as shown in Figure 1. Design and as-built layer thicknesses are summarized in Table 1. As-built pavement thicknesses were obtained from measurements in a trench in the non-trafficked area excavated following completion of the HVS trafficking.

Table 1 Pavement Layer Thicknesses for Test 545

Layer	Design (mm)	As Built (mm)
Dense Graded Asphalt Concrete	75	90
Asphalt Concrete	148	143
Aggregate Base	182	259
Aggregate Subbase	215	206-280

2.2 Environmental Conditions

The accelerated pavement test was conducted under wet conditions at moderate pavement temperatures. The design water inflow into the pavement was 9.7 liters per hour over an area 7.4 m wide by 12 m long to simulate an average peak week precipitation in Eureka, CA of 51.3 mm. Since the rate of water infiltration into the aggregate base was lower than the design water inflow, the water inflow was reduced accordingly to approximately 0.4 liters per hour.

The water was introduced through a line of holes parallel to and upslope from the HVS test section. An electronic valve and timer system continuously controlled water inflow to the pavement during the test. Reference (*3*) contains photographs of the system.

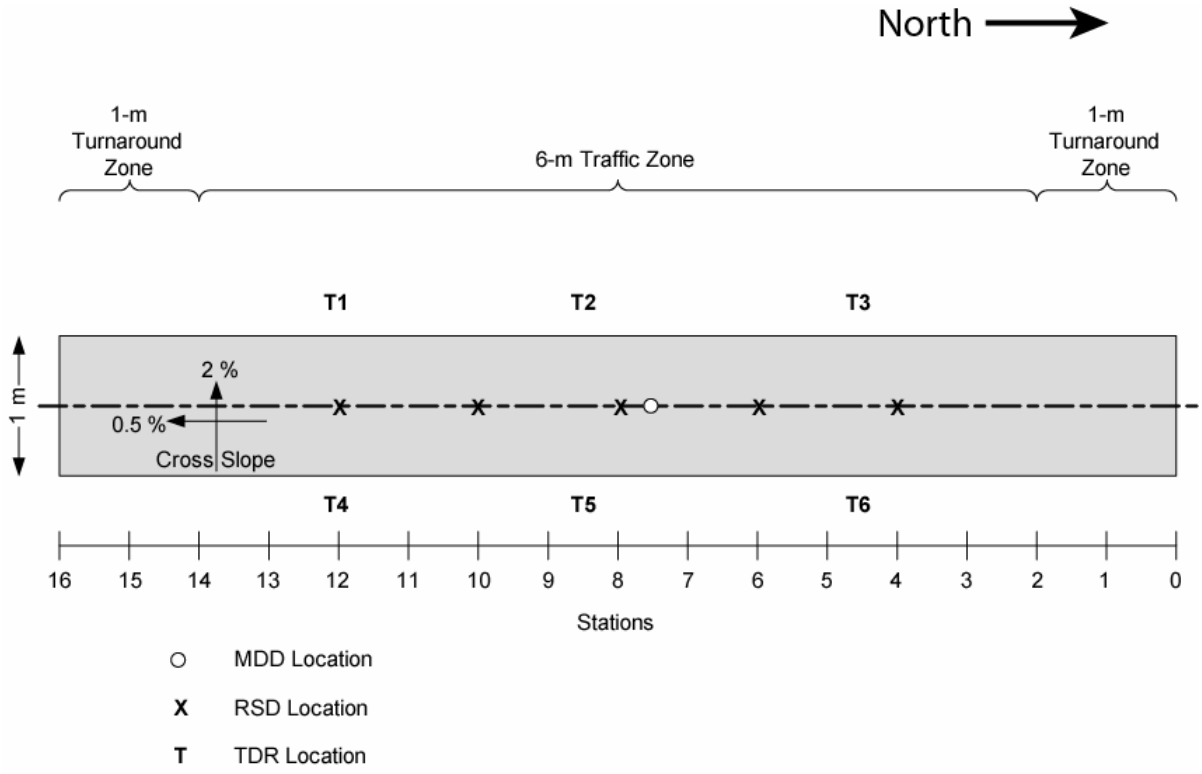

Figure 1. Test section layout and instrumentation.

The target pavement temperature at a pavement depth of 50 mm was 20ºC ± 2 °C. In contrast to Sections 543 and 544, Section 545 did not utilize a temperature control box during testing. If pavement temperatures were not within the specified range, HVS testing was stopped until the temperature was back within the desired range.

2.3 Instrumentation

The instrumentation used in Section 545 included 1) Multi-Depth Deflectometers (MDD) to measure deflections and permanent deformations at various depths in the pavement section, 2) laser profilometer to monitor surface rutting, 3) Road Surface Deflectometer (RSD) to measure surface deflections, 4) thermocouples to monitor pavement temperatures, and 5) Time Domain Reflectometers (TDR) to monitor moisture content in the unbound layers.

Figure 2 shows the vertical location of MDDs and thermocouples in Section 545. Figure 1 shows the section layout and location of RSD, MDD, and laser profilometer measurements. Reference (*4*) contains a complete description of the instrumentation used for this study.

2.4 Test Program

Evaluation of the test section performance was accomplished in four stages (Figure 3).

- Stage 1: Testing and evaluation of the pavement section prior to water infiltration. Water measurements and FWD testing were conducted to establish initial conditions and structural capacity.
- Stage 2: Testing and evaluation of pavement section during water infiltration. Water measurements and FWD testing were conducted to establish conditions and structural capacity prior to HVS testing.
- Stage 3: HVS testing with water infiltration of the pavement. During loading, the pavement section was monitored using the instrumentation noted in Section 2.3.
- Stage 4: Evaluation of the pavement section at the conclusion of HVS trafficking by means of FWD testing, trenching, and sampling of the pavement materials. Trenching and sampling of the materials were conducted simultaneously with the forensic activities on Section 544.

2.4.1 Heavy Vehicle Simulator Trafficking

For trafficking of Section 545, the HVS was equipped with dual truck tires, representing one-half of a single axle. Load was applied through two Goodyear radial tires (G159 11R 22.5) inflated to a pressure of 720 kPa. Three load levels were used; Table 2 summarizes the loading sequence.

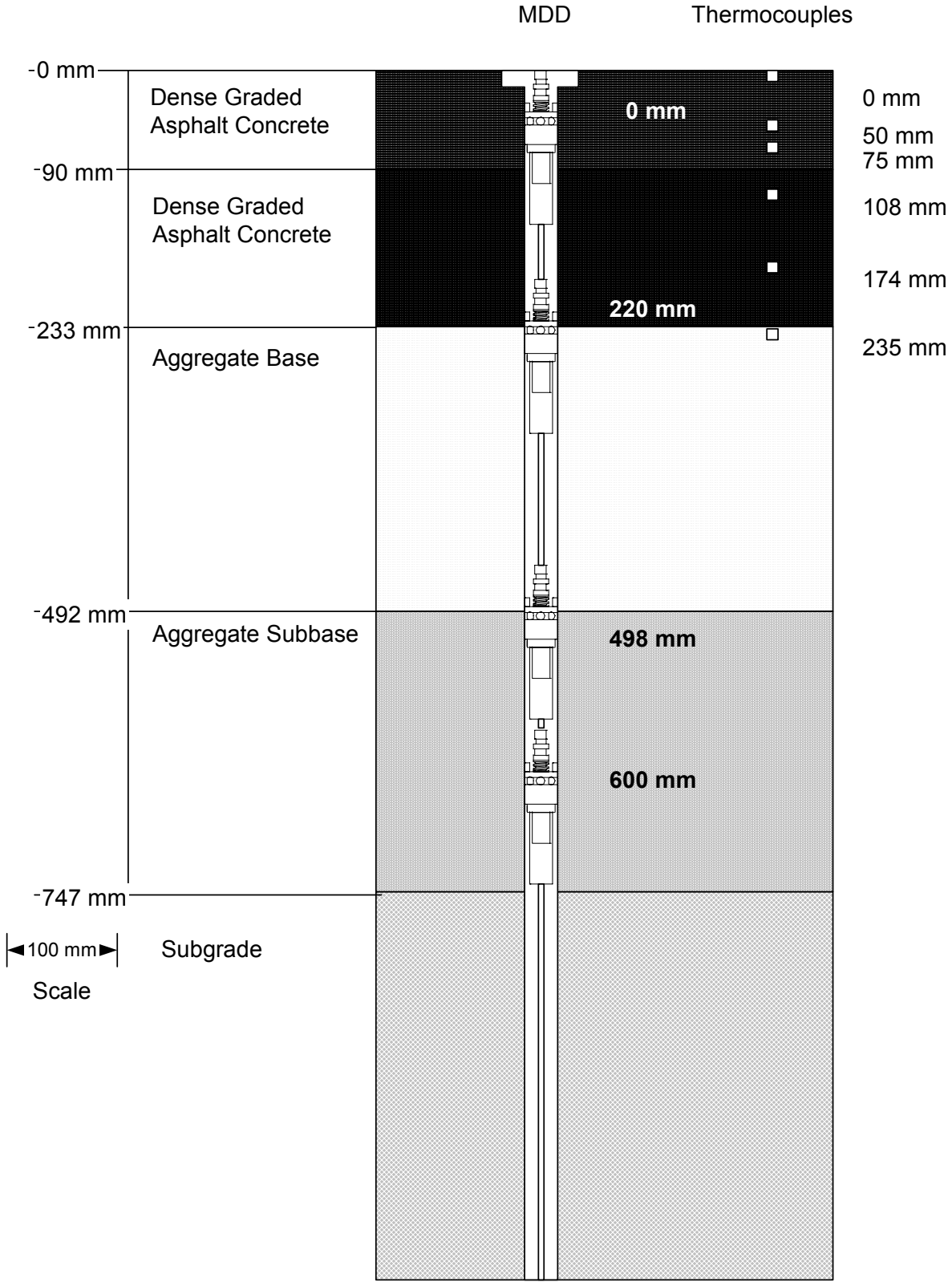

Figure 2. Location of MDDs and thermocouples in Section 545.

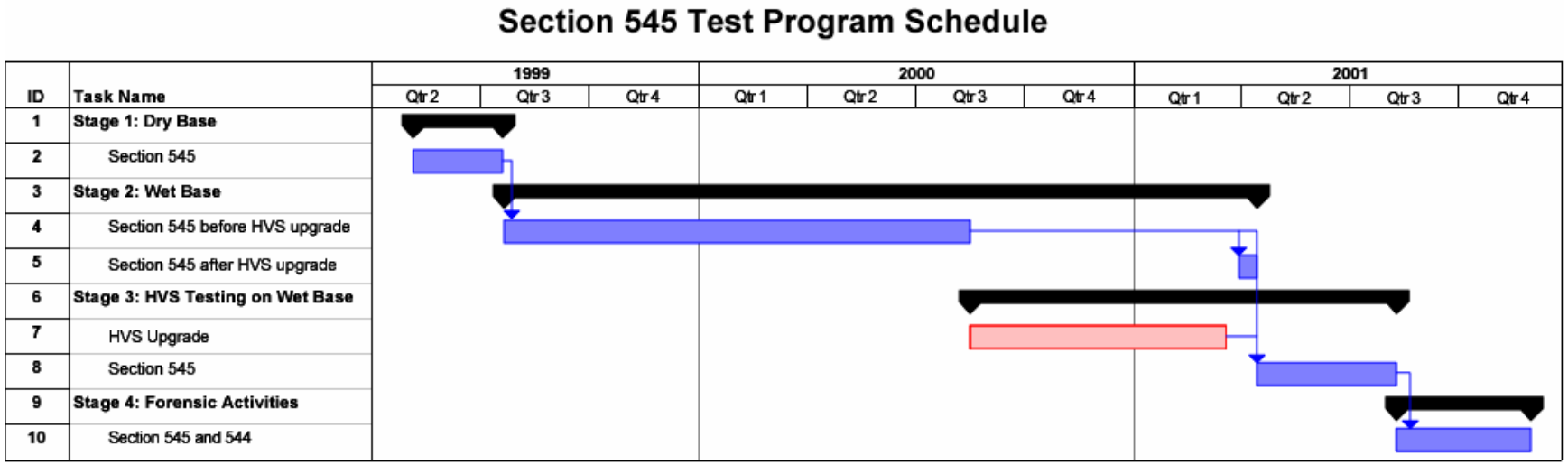

Figure 3. Section 545 test program schedule.

Table 2 Applied Trafficking Loads in Section 545

Trafficking Load (kN)	HVS Repetitions
40	0 to 147,000
80	147,000 to 264,612
100	264,612 to 741,922

The test wheel trafficked the entire length of the 8-m test section. Lateral wander over the 1-m width of the test section was programmed to simulate traffic wander on a typical highway lane. Pavement performance was evaluated for the 6 m × 1 m area between reference points 2 and 14 in which the HVS wheel speed is constant. The 1-m^2 areas at both ends of the trafficked area (Stations 0–2 and 14–16) serve as "turnaround zones" in which the test wheel decelerates, accelerates, and changes direction (Figure 1).

2.4.2 Data Collection

Table 3 summarizes the data collection sequence for Section 545.

Table 3 Data Collection Program

Load Applications	Laser Profilometer	Multi-Depth Deflectometer	Road Surface Deflectometer	Crack Monitoring
10	X	40 kN	40 kN	
15000	X	40 kN	40 kN	
50000	X	40 kN	40 kN	
90000	X	40 kN	40 kN	
116000	X	40 kN	40 kN	
147000	X	40 kN	40 kN	
187767	X	40, 80 kN	40, 80 kN	
216000	X	40 kN	40 kN	
249000	X	40, 80 kN	40, 80 kN	
264612	X	40 kN	40 kN	
300000	X	40 kN	40 kN	
323314	X	40, 80 kN	40, 80 kN	
383692	X	40 kN	40 kN	
427000	X	40 kN	40 kN	X
482000	X	40, 80, 100 kN	40, 80, 100 kN	
517000	X	40 kN	40 kN	X
551663	X	40, 80, 100 kN	40, 80, 100 kN	X
741922	X	40, 80, 100 kN	40, 80, 100 kN	X

3.0 SUMMARY OF TEST DATA

This chapter provides a summary of the test data collected for the four stages of testing. The data include:

- Stage 1 and 2: Temperature, water content, and FWD data.
- Stage 3: Temperature, water content, permanent deformation, elastic deflection, and crack measurements.
- Stage 4: FWD and forensic data.

3.1 Temperature and Moisture Condition Data

Temperature and moisture condition data were obtained throughout testing of Section 545. The following sections summarize these data.

3.1.1 Temperature

Figure 4 shows daily average air temperatures in building 280 at the University of California Berkeley Richmond Field station where the HVS was located, and daily average pavement temperatures at several depths. The daily average temperatures were calculated from hourly temperatures recorded during testing. The average air temperature at the test section was 19ºC with a standard deviation of 2.2°C. As noted earlier, Section 545 was tested without the temperature control box.

Asphalt concrete temperatures were recorded at various depths in the asphalt concrete layers as seen in Figure 4. Asphalt concrete temperatures were fairly uniform and varied slightly with air temperature on the test section. In general, average temperatures in the asphalt concrete layers were slightly higher than the average air temperatures (19.5ºC versus 19.0ºC).

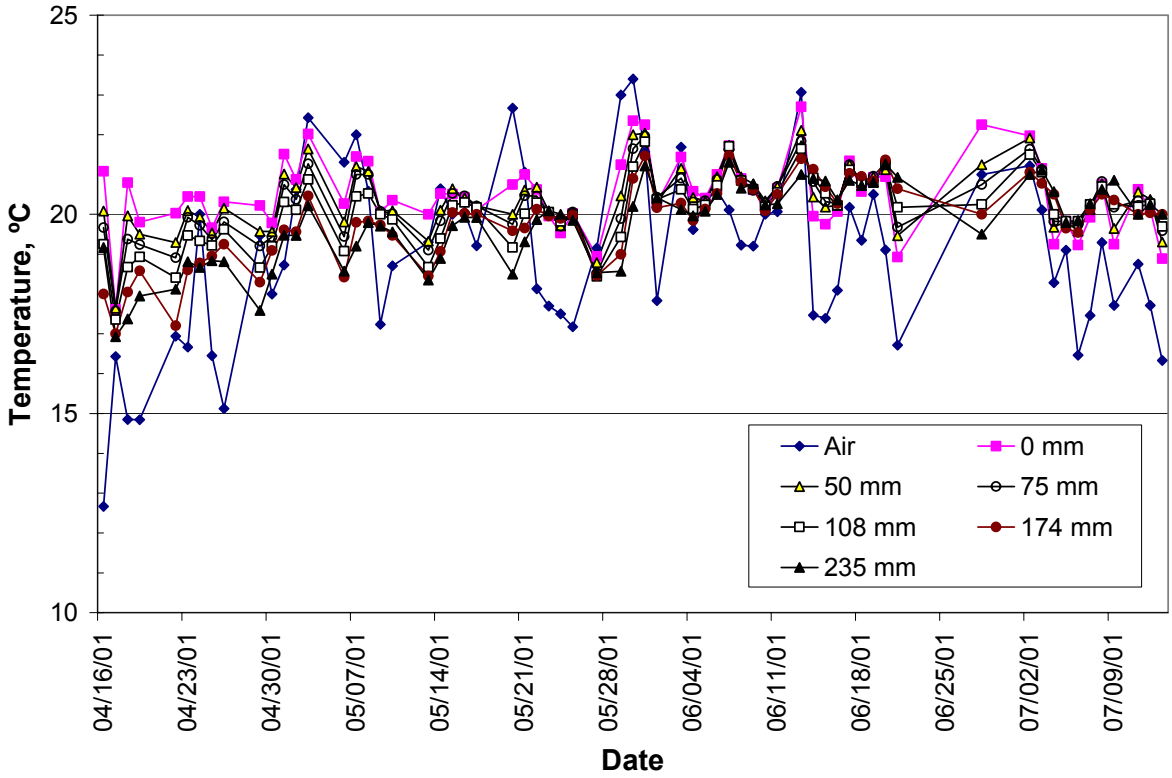

Figure 4. Average air and in-pavement temperatures during trafficking of Section 545.

3.1.2 Rainfall

Figure 5 shows average monthly rainfall data from the National Weather Service weather station in Richmond, CA during the four stages of testing.

3.1.3 Moisture Content Data

Moisture contents were measured using hydrorobes and Time Domain Reflectometers. Data obtained with both types of equipment are summarized in the following sections.

3.1.3.1 Hydroprobes

Figures 6 and 7 illustrate average volumetric moisture contents for the aggregate base, subbase, and subgrade materials obtained by using a hydroprobe test device. Hydroprobe

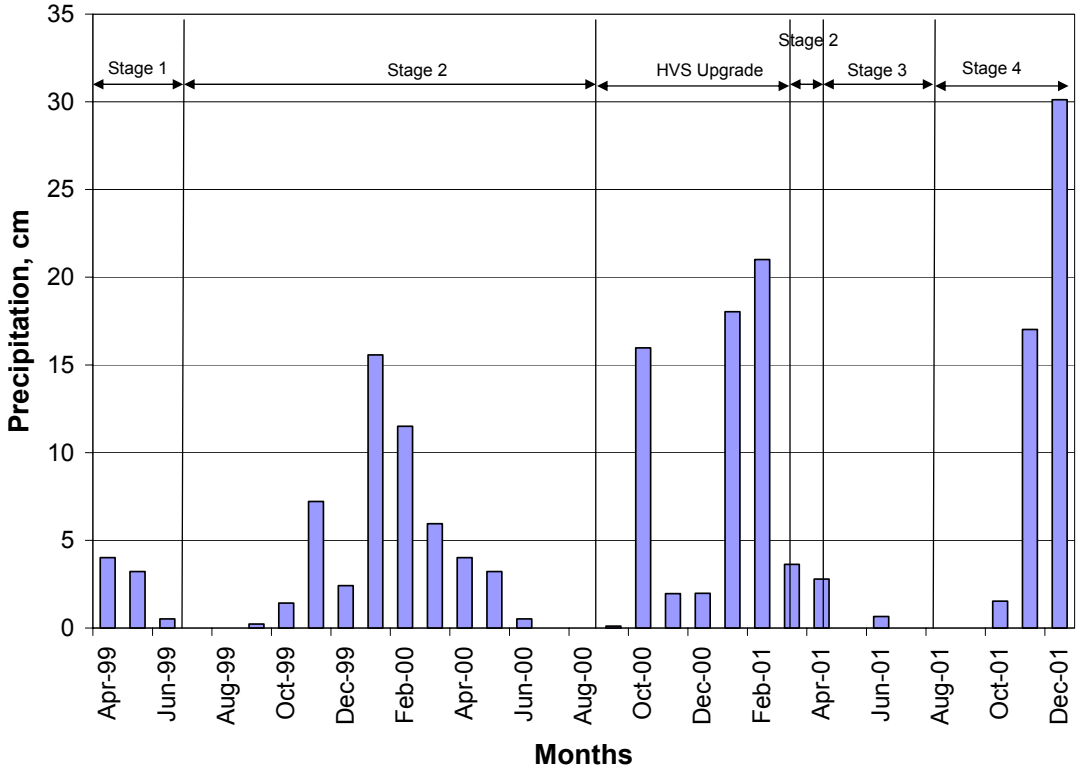

Figure 5. Monthly precipitation for Richmond weather station.

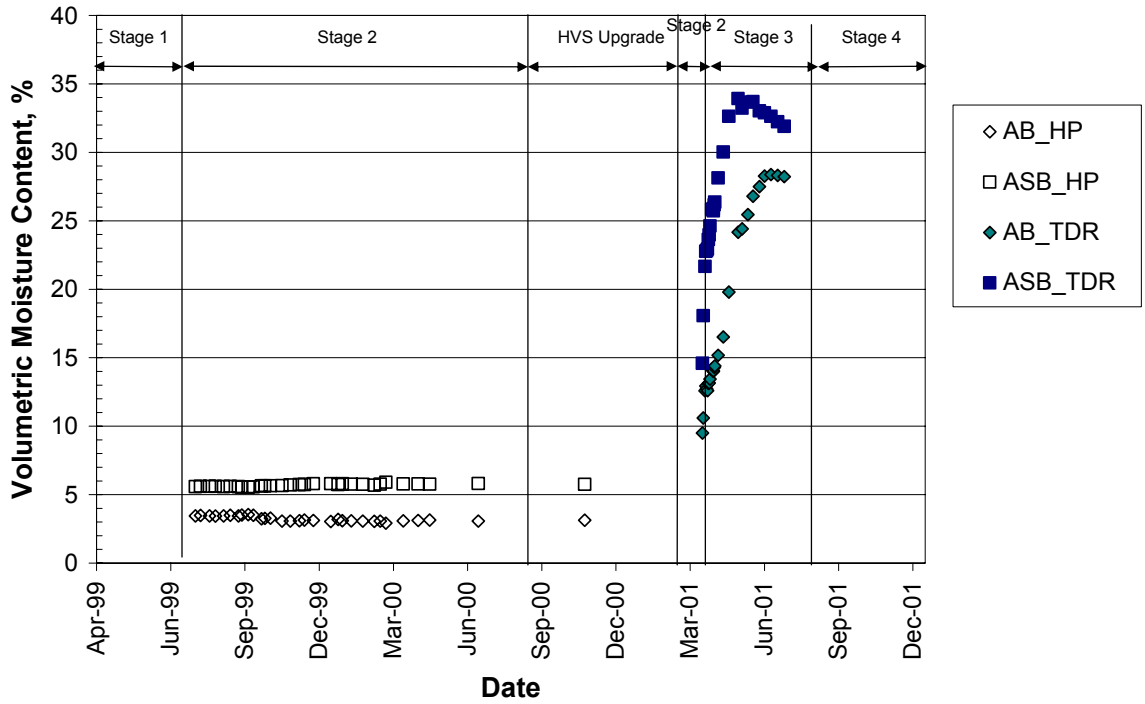

Figure 6. Average volumetric moisture contents for the aggregate base and subbase obtained with hydroprobes and TDRs.

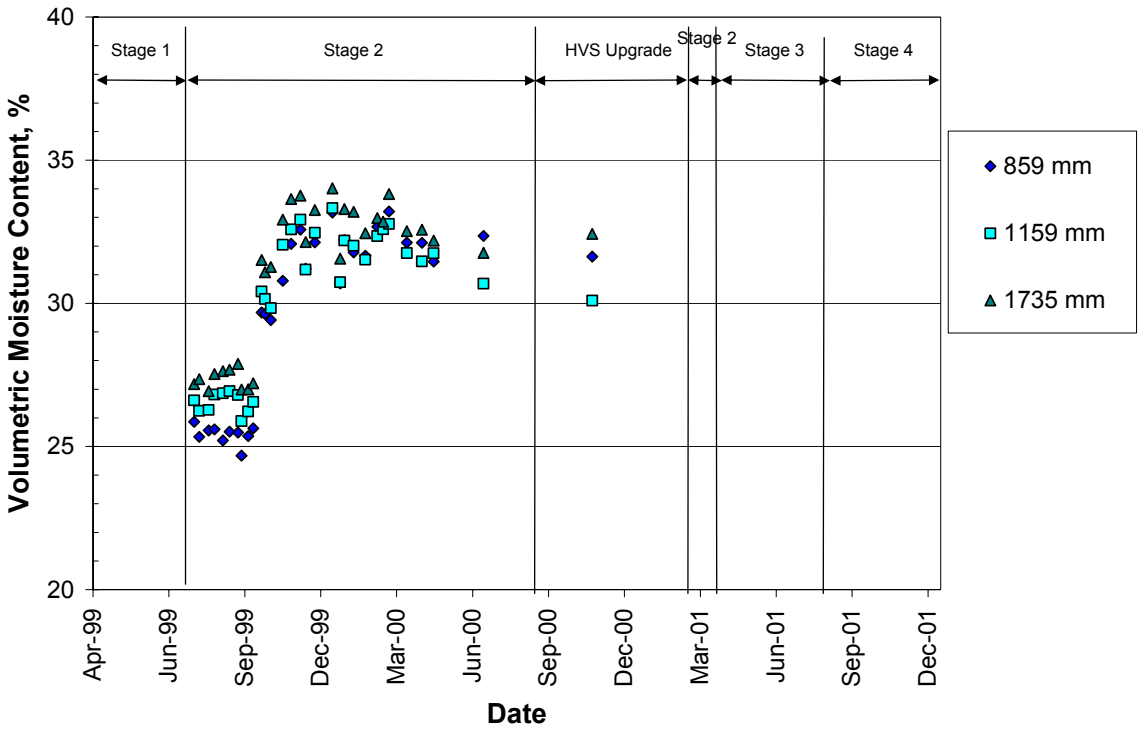

Figure 7. Average volumetric moisture contents for the subgrade obtained with the hydroprobe.

readings for the aggregate base and subbase were taken at depths of 320 mm and 586 mm from the pavement surface. Hydroprobe readings for the subgrade were taken at a pavement depth of 859 mm, 1159 mm, and 1735 mm.

Volumetric moisture contents of the base and subbase were averaged across measurements taken for those layers. Figure 6 shows that the moisture contents of these two layers remained constant through all stages of testing. Moisture contents were expected to increase at least in the aggregate base due to water infiltration.

Moisture content data for the subgrade exhibit variations which followed the precipitation trends during the testing (Figure 5). This was expected since the subgrade at the test site was not isolated from the surrounding soil.

3.1.3.2 Time Domain Reflectometers

Time Domain Reflectometers (TDR) were installed in Section 545 to verify the measurements obtained with the hydroprobe device in the aggregate base layers. Figure 6 shows average volumetric moisture content measurements for the aggregate base and subbase layers. Measurements were taken at six locations as indicated in Figure 2. TDRs were installed vertically to measure the moisture content across the thickness of the layers. TDR data indicate moisture content changes in the aggregate base and subbase due to the infiltrated water. These changes were not observed with the hydroprobe device, as noted earlier.

For this test sections, the increased moisture contents in the base and subbase reflected by the TDR measurements correspond with the reduced stiffnessess of those materials which occurred in situ. It is expected the hydroprobe was not functioning properly thereby leading to values which were inconsistent with the material stiffnesses and other moisture data reported in Reference (*3*).

3.2 Permanent Deformation

Permanent deformation data were obtained using the laser profilometer and multi-depth deflectometers (MDDs). The following sections summarize these data.

3.2.1 Surface Rutting Measured with the Laser Profilometer

Figure 8 shows accumulated average maximum rut depth for Section 545. A rapid rate of permanent deformation is noted under the 40-kN trafficking load during the first load applications with no significant accumulation of rutting until application of the 80- and 100-kN trafficking loads. Table 4 summarizes average rates of rutting for each of the three levels of traffic loading.

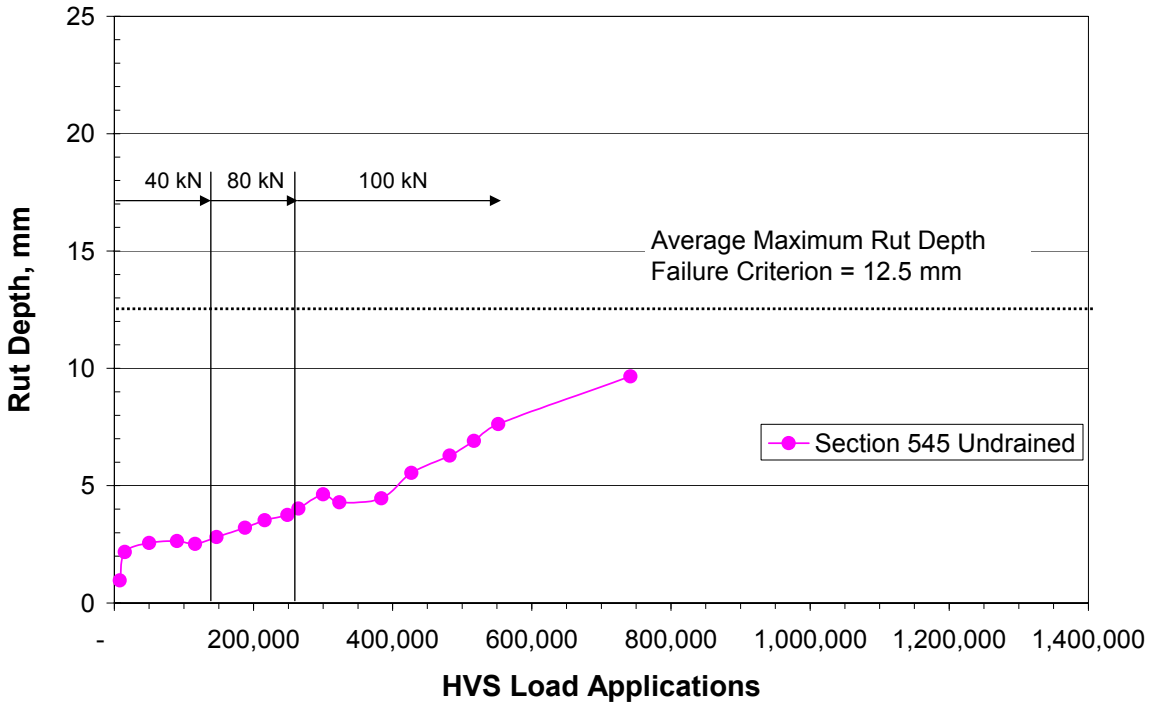

Figure 8. Average maximum rut depth.

Table 4 Average Rate of Rutting in Section 545

Load	Rate of Rutting (mm/million load repetitions)
40 kN	14.4*
80 kN	9.2
100 kN	11.8

*While this rate is higher than that for the 80- and 100-kN loads, it must be emphasized that much of the deformation occurred under a relatively few repetitions, i.e., approximately 2 of the 2.5 mm obtained under the 40-kN load.

Figure 9a–9c shows the rut depth distributions at the end of the 40-, 80-, and 100-kN trafficking loads, respectively. Rut distributions are fairly uniform throughout the section with greater rutting localized around Station 8. The center of the HVS wheelpath corresponds to 0 mm transverse distance; the rut depths are given in millimeters.

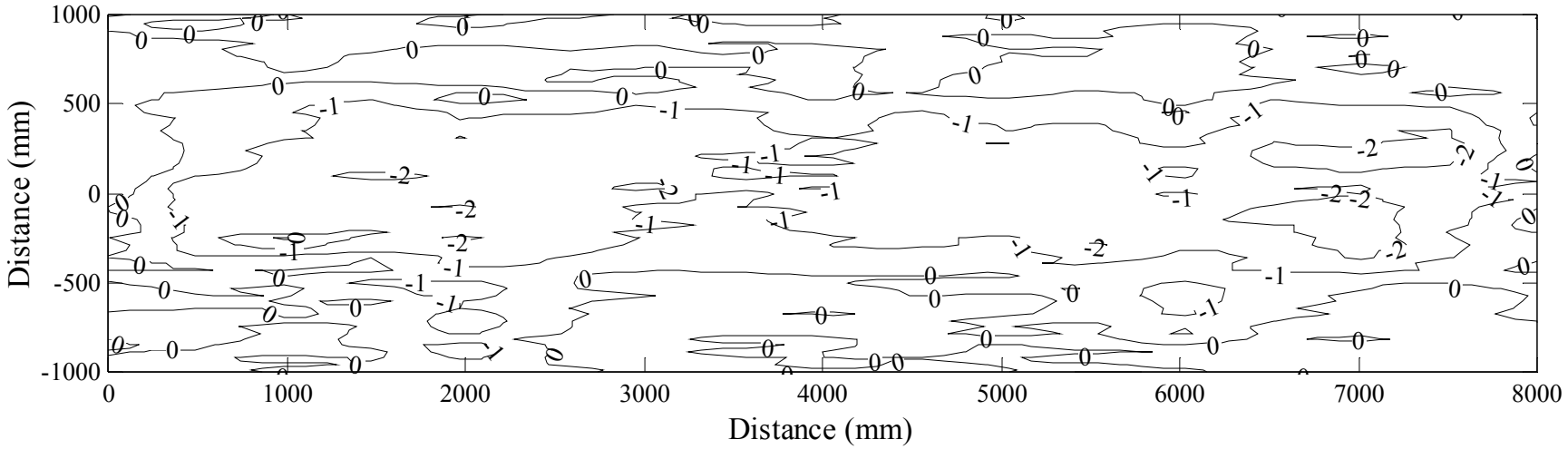

Figure 9a. Section 545 surface profile, 147k repetitions.

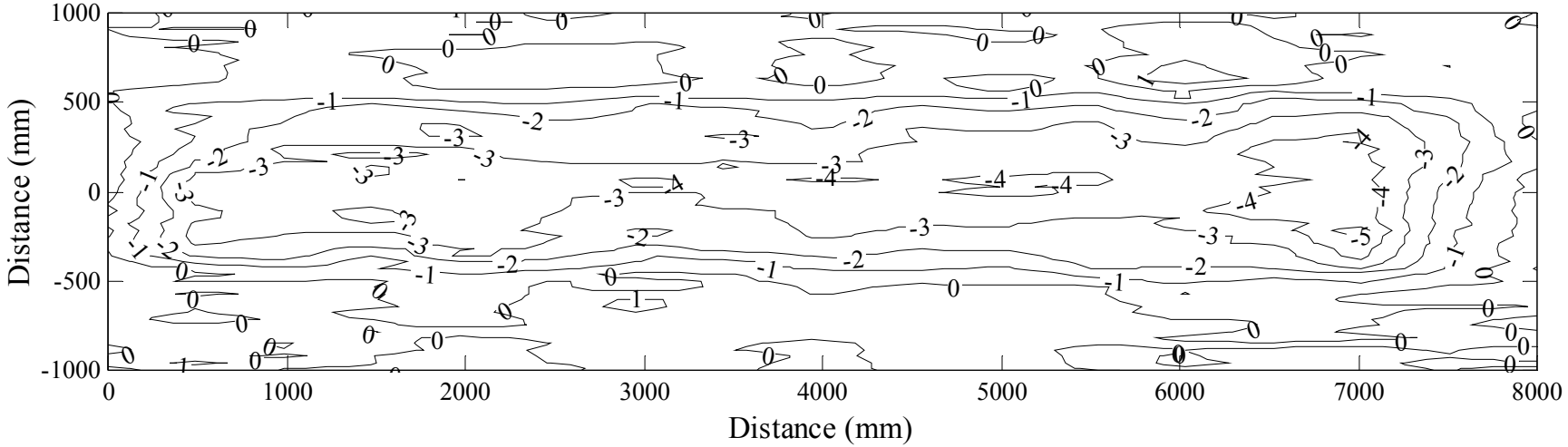

Figure 9b. Section 545 surface profile, 384k repetitions.

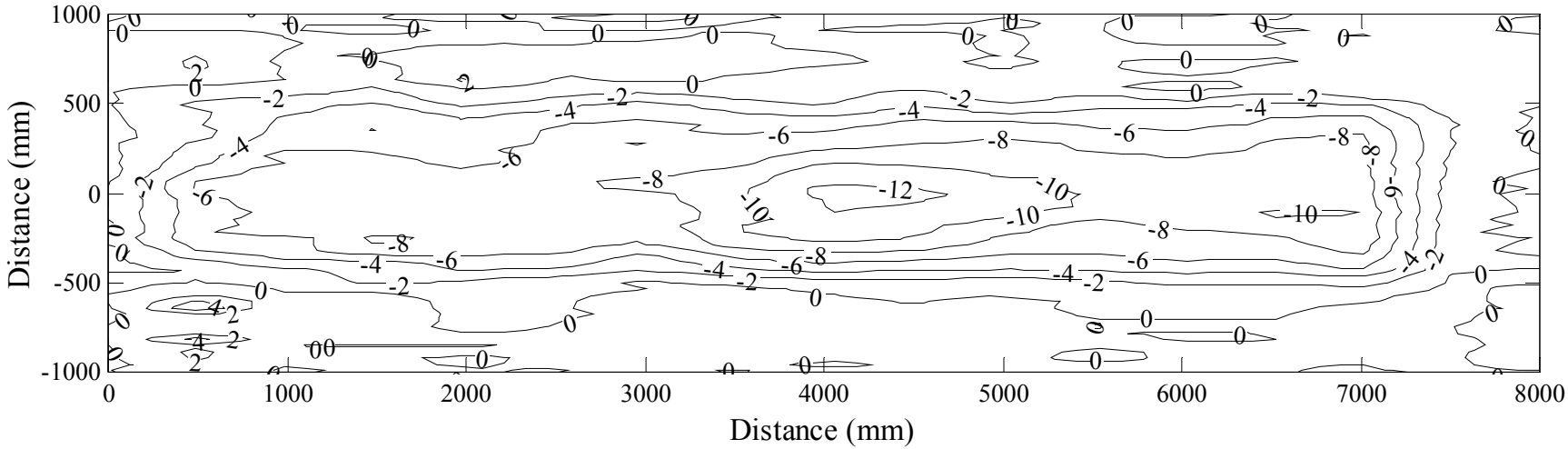

Figure 9c. Section 545 surface profile, 742k repetitions.

Figure 9. Section 545 surface profile at various stages of HVS trafficking.

3.2.2 In-depth Permanent Deformation

Figure 10 shows the permanent deformation recorded at various depths in the test section using the MDDs installed near Station 7 (refer to Figure 1 for instrument depths). The deformation data at the subgrade level are not presented because the two MDD modules installed at those depths did not function properly.

The rapid increase in permanent deformation with load applications is evident for all the layers under the 80- and 100-kN load.

Figure 11 summarizes the development of permanent deformation in each layer. Note that it was not possible to separate permanent deformation occurring in the subbase and subgrade. Table 5 summarizes the average contributions of the asphalt concrete, aggregate base, and aggregate subbase/subgrade to permanent deformation during loading. These contributions are based on MDD data illustrated in Figure 10. Of particular importance is the proportionate increase in permanent deformation in the untreated aggregate base, which can be attributed to the increase in stress in this layer and its reduced stiffness due to increase moisture content.

Table 5 Contribution in Percent of Pavement Component to Surface Rutting

Pavement Component	Stage of Testing Based on Trafficking Loads		
	40 kN	80 kN	100 kN
Asphalt Layers	43	48	16
Aggregate Base	44	40	74
Aggregate Subbase and Subgrade	13	11	10

3.2.3 Comparison with Section 544

Sections 545 and 544 were tested under similar conditions. That is, both contained untreated bases (undrained) which were saturated prior to testing, as described in Section 2 of this report. The difference between the two sections was in the type of overlay. Section 544

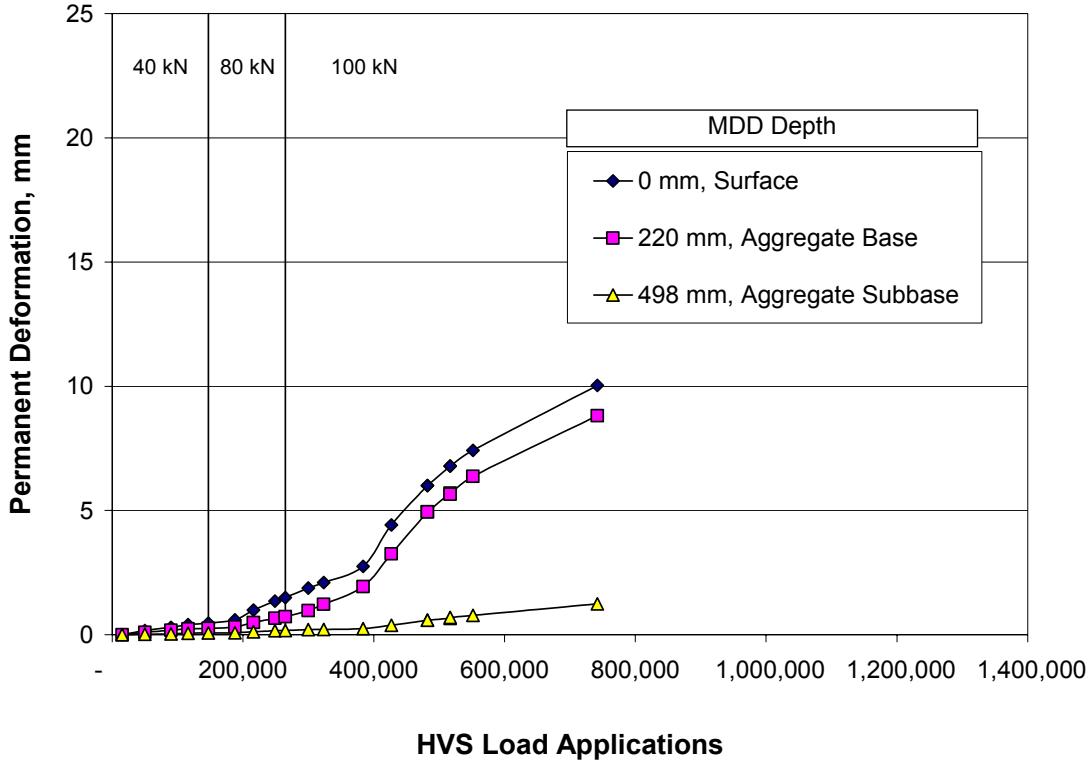

Figure 10. In-depth permanent deformations in Section 545 near Station 7.

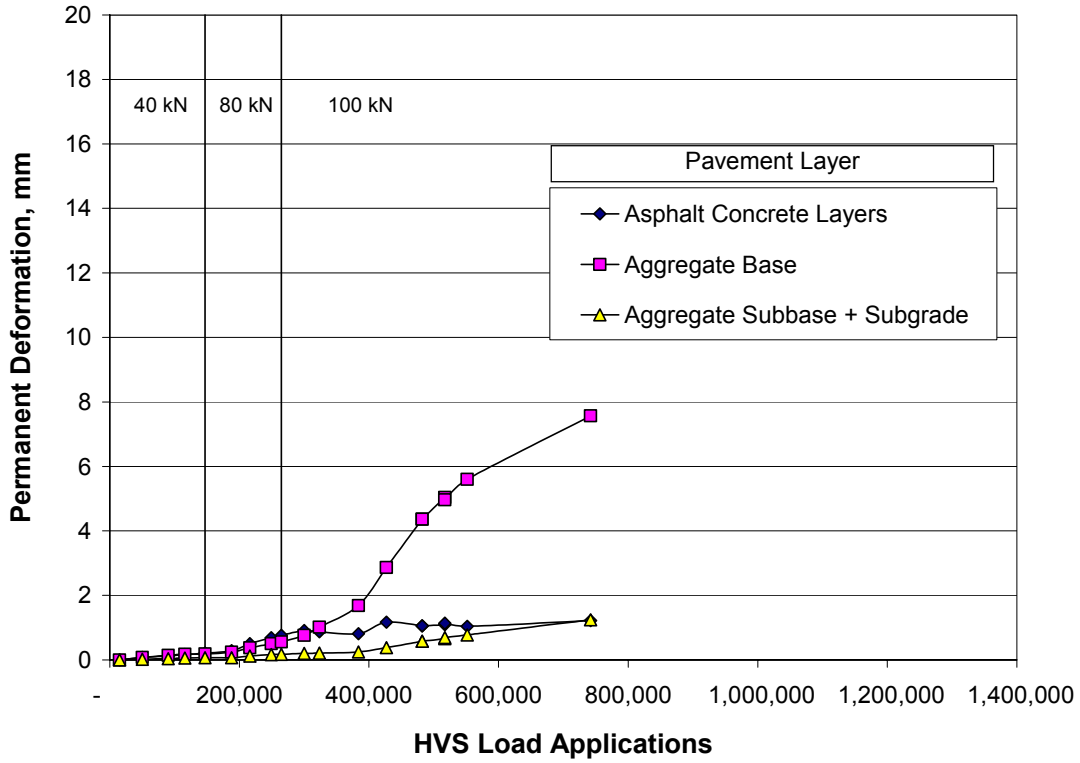

Figure 11. Permanent deformation within pavement lyaers in Section 545 near Station 7.

contained a 51-mm thick ARHM-GG surface course whereas Section 545 was surfaced with a 90-mm thick conventional DGAC mix. Figure 12 contains a summary of the permanent deformations occurring in the AC surface layers, the untreated base, and the subbase/subgrade combination for both test sections.

In Figure 12, it will be noted that permanent deformations contributed by the subbase/subgrade combination are similar for the two sections. However, the permanent deformation in the AC layer is higher in Section 544 than Section 545 while the reverse is true for the saturated untreated base courses under the 100-kN loading. This difference suggests that the local stresses in the base of Section 545 were likely higher and/or the base stiffness was less as compared to the base for Section 544. Comparisons of the elastic deformations for the two base courses to support such a hypothesis, as discussed in Section 3.3

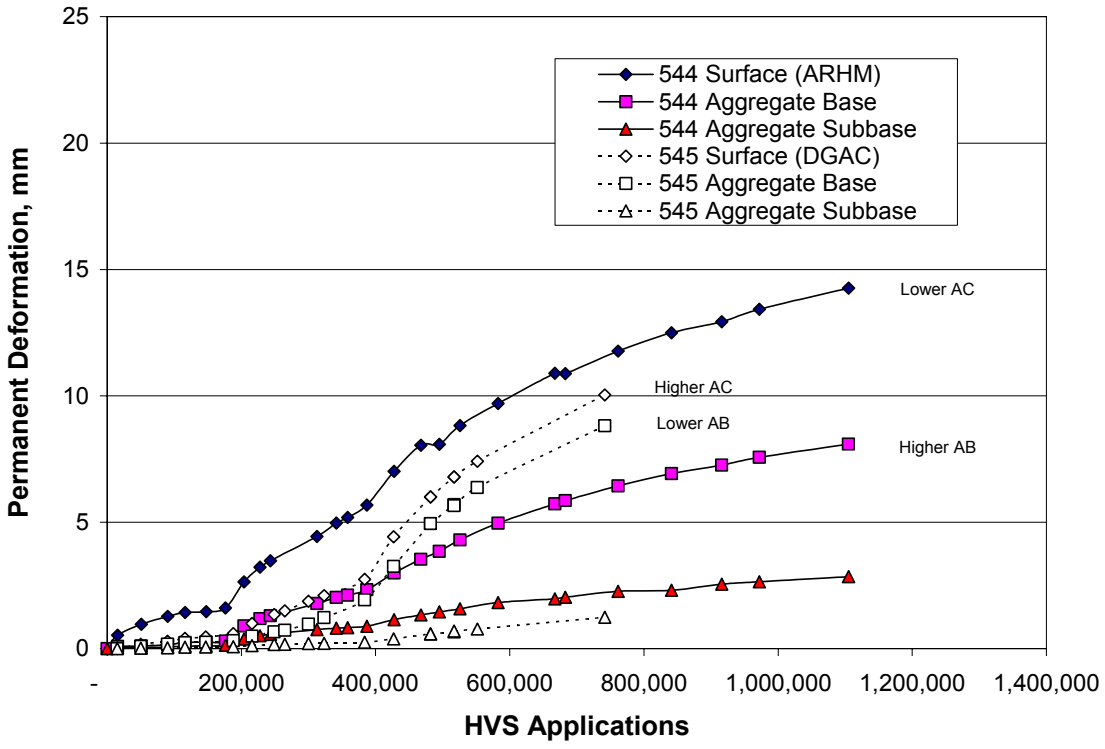

Figure 12. Comparison of permanent deformations on Sections 544 ad 545.

3.3 Elastic Deflections

Elastic deflections in the pavement sections were measured with the Road Surface Deflectometer (RSD) and MDDs. Surface and in-depth deflection data presented in the following sections are peak values obtained from the deflection basins.

3.3.1 Surface Deflection Data

Surface elastic deflections were monitored using the RSD along the section centerline at Stations 4, 6, 8, 10, and 12 under the 40-, 80-, and 100-kN test loads. Figure 13 shows average deflection data for the three test loads. Considering the measurements with the 40-kN load in this figure, it will be noted that the elastic deflections increased with successive load applications with significant increases as the trafficking load was increased from 40 kN to 80 kN and then to

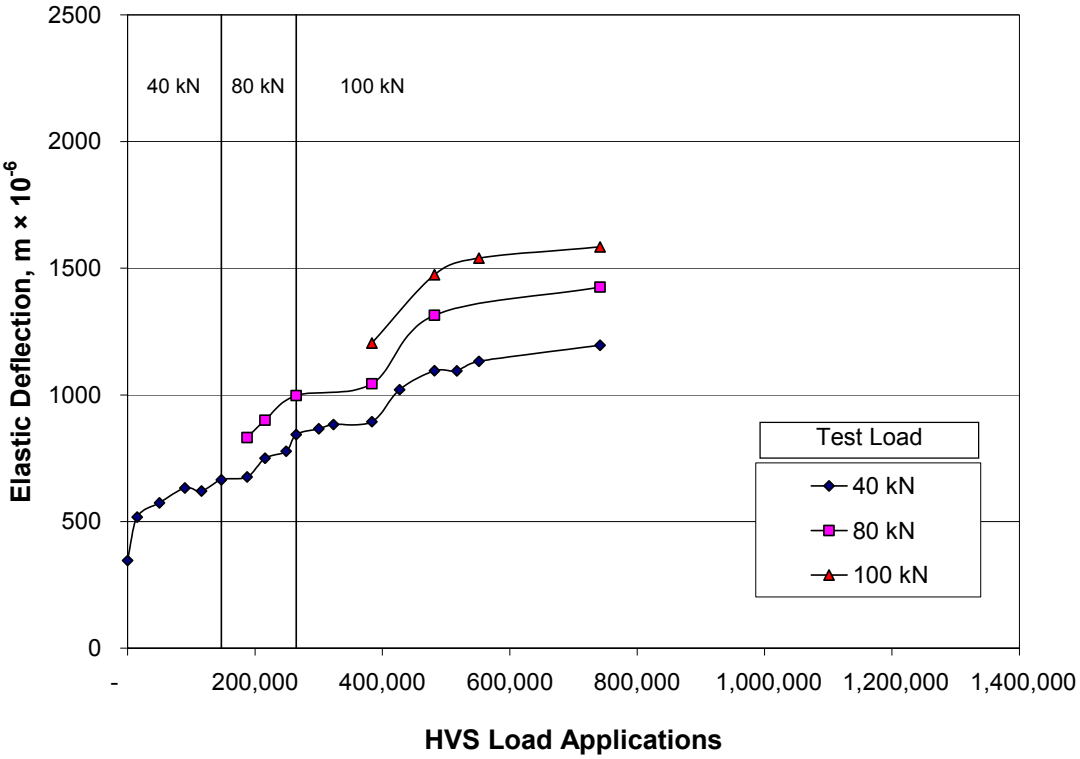

Figure 13. Average RSD deflections for Section 545.

100 kN. These measurements suggest that cracking developed in the asphalt concrete with damage developing progressively with increased repetitions.

Figure 14 shows RSD deflections along Section 545 at the completion of HVS testing. The data indicate that the elastic response was reasonably uniform throughout the section with coefficients of variation for the elastic deflections associated with the 40-, 80-, and 100-kN test loads of 6, 6, and 5 percent respectively.

3.3.2 In-Depth Pavement Deflections

In-depth elastic deflection data under the 40-, 80-, and 100-kN test loads are presented in Figures 15, 16, and 17. Increases in elastic deflections were recorded with HVS trafficking for all layers under all test loads. The data indicate that the unbound layers yielded the highest elastic deflections. The rate of increase of the elastic deflections leveled off at about 470,000 HVS load

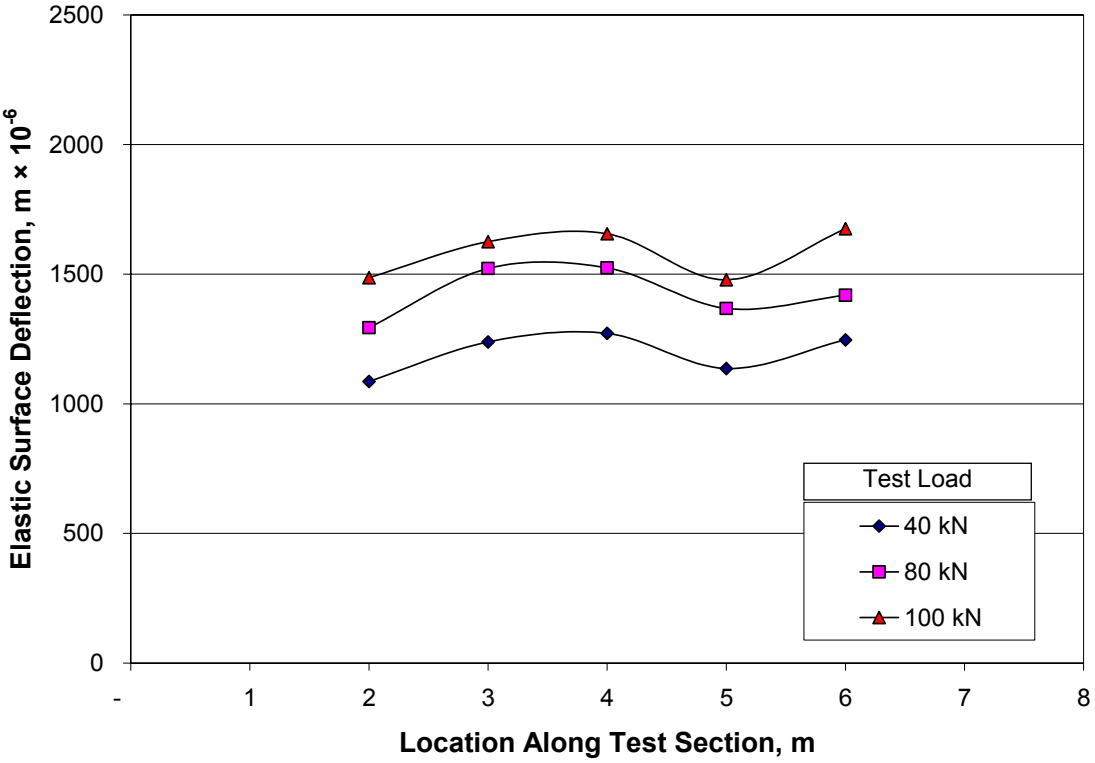

Figure 14. RSD at the end of testing, 741,922 load applications.

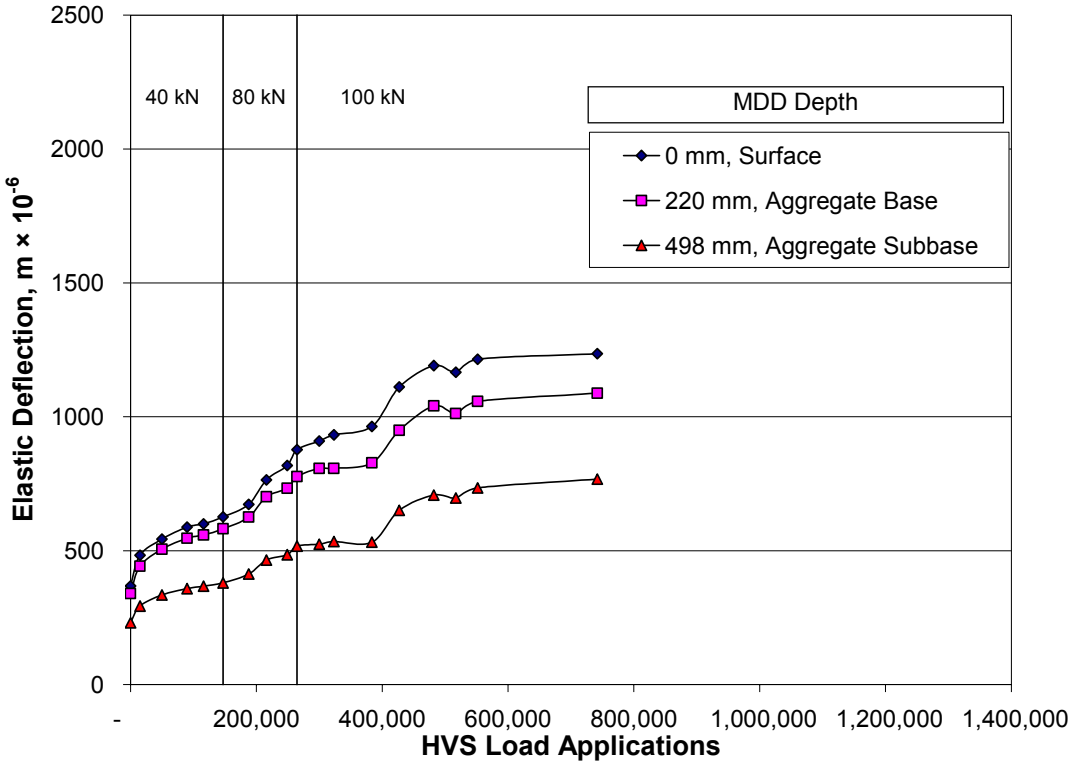

Figure 15. In-depth elastic deflections resulting from 40-kN test load, MDD 7.

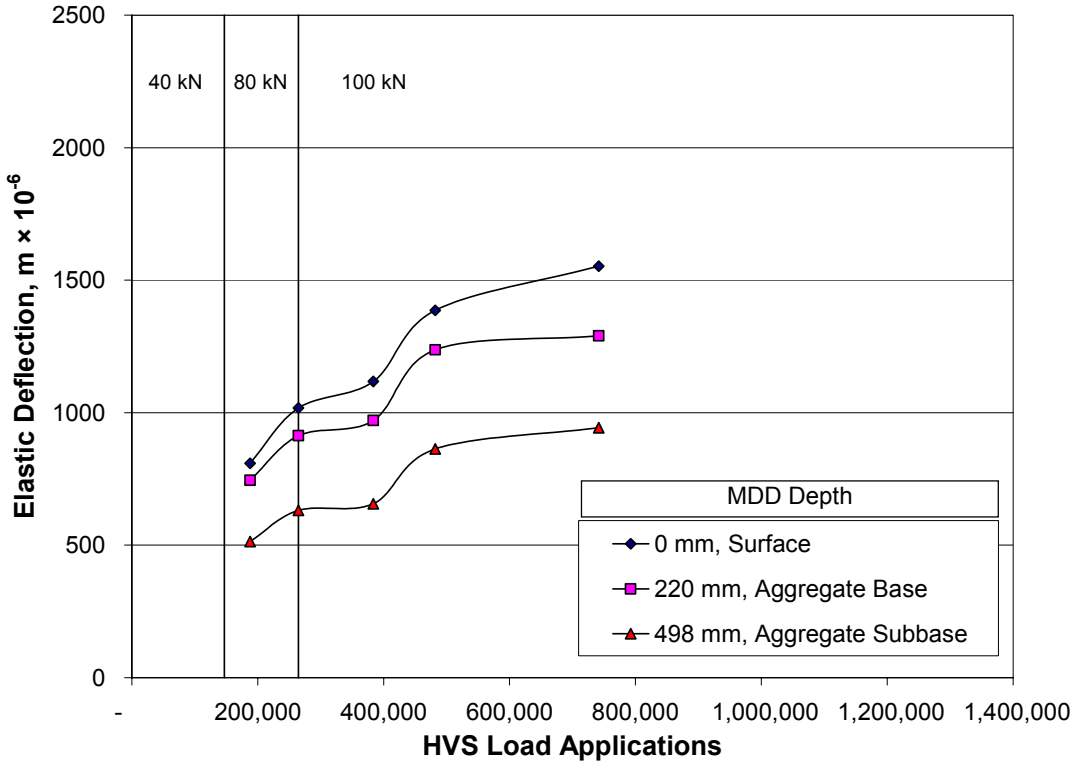

Figure 16. In-depth elastic deflections resulting from 80-kN test load, MDD 7.

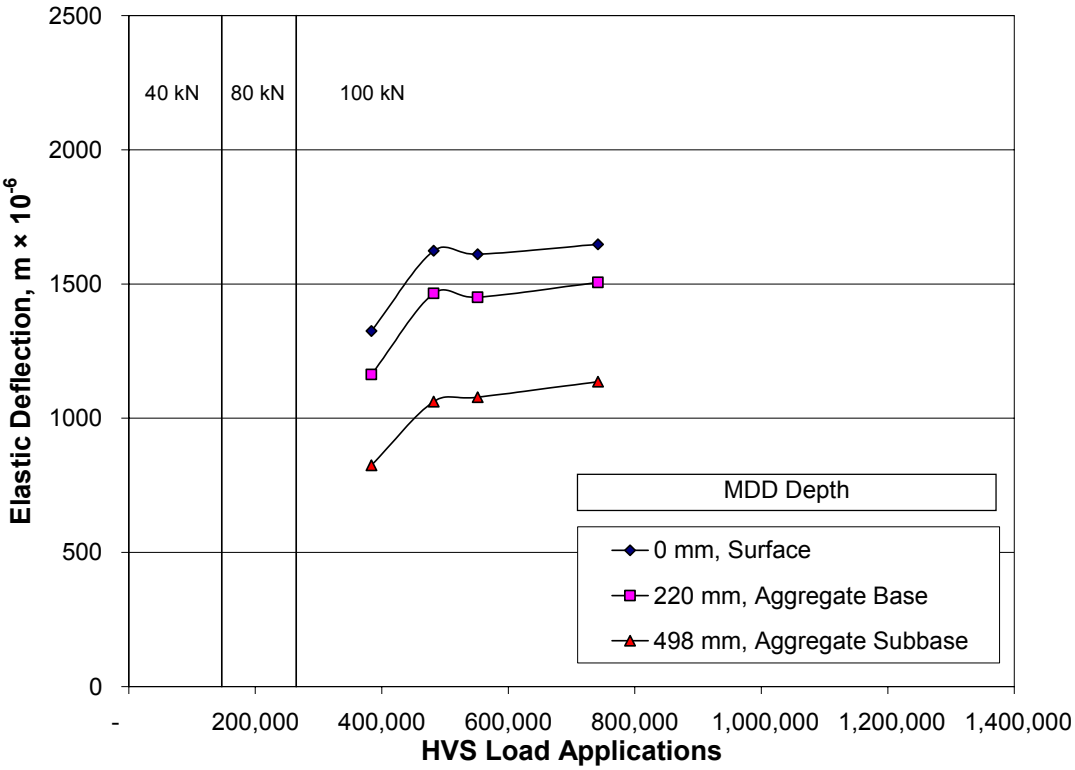

Figure 17. In-depth elastic deflections resulting from 100-kN test load, MDD 7.

applications. This leveling off in elastic deflections occurred at about the same time that cracks appeared at the pavement surface.

Elastic deflections occurring in each of the layers under the 40-, 80-, and 100-kN loads are summarized in Figures 18, 19, and 20 respectively. Table 6 contains a summary of the average percent contribution of the various pavement layers to the total surface elastic deflections. In these figures, as well as in Table 6, it will be noted that the majority of the elastic deflections measured at the surface were contributed by the subbase/subgrade combination (53 to 64 percent depending on the applied load).

Table 6 Contribution in Percent to Surface Elastic Deflection of Pavement Components

Pavement Component	Test Load					
	40 kN			80 kN		100 kN
	Trafficking Load					
	40 kN	80 kN	100 kN	80 kN	100 kN	100 kN
Asphalt Layer	2	7	14	5	11	10
Aggregate Base	44	40	33	33	27	27
Aggregate Subbase and Subgrade	54	53	53	62	62	64

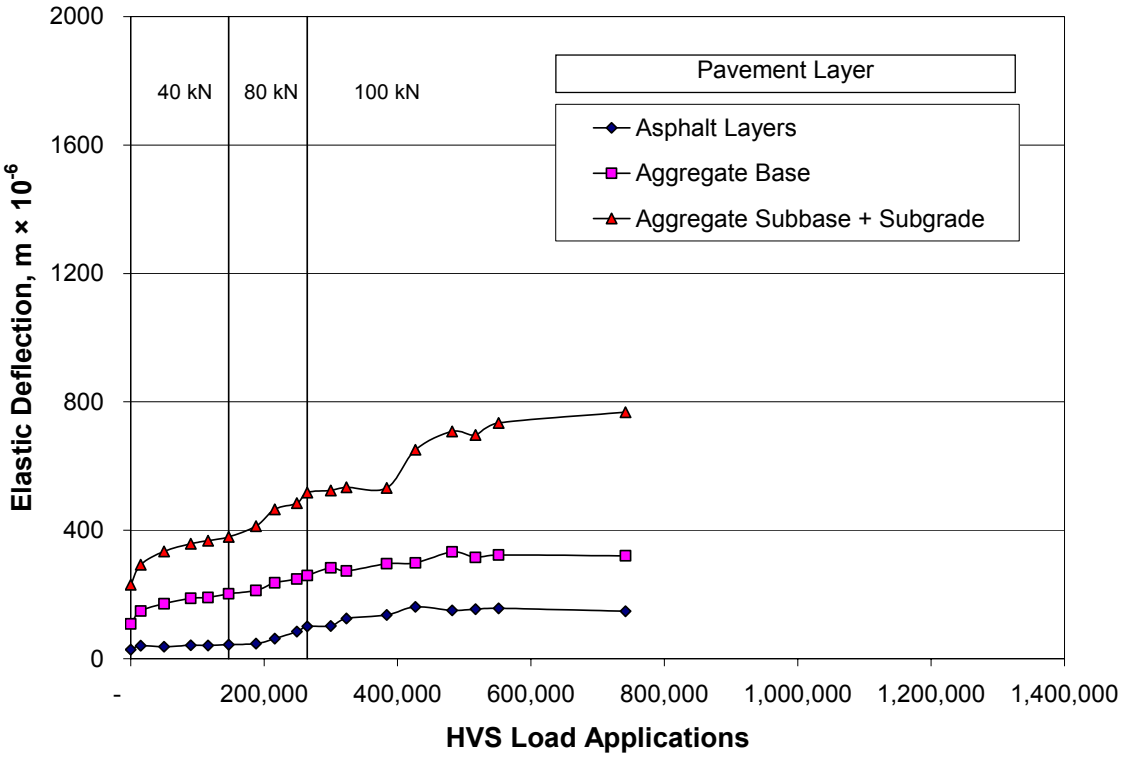

Figure 18. Layer elastic deflections resulting from 40-kN test load.

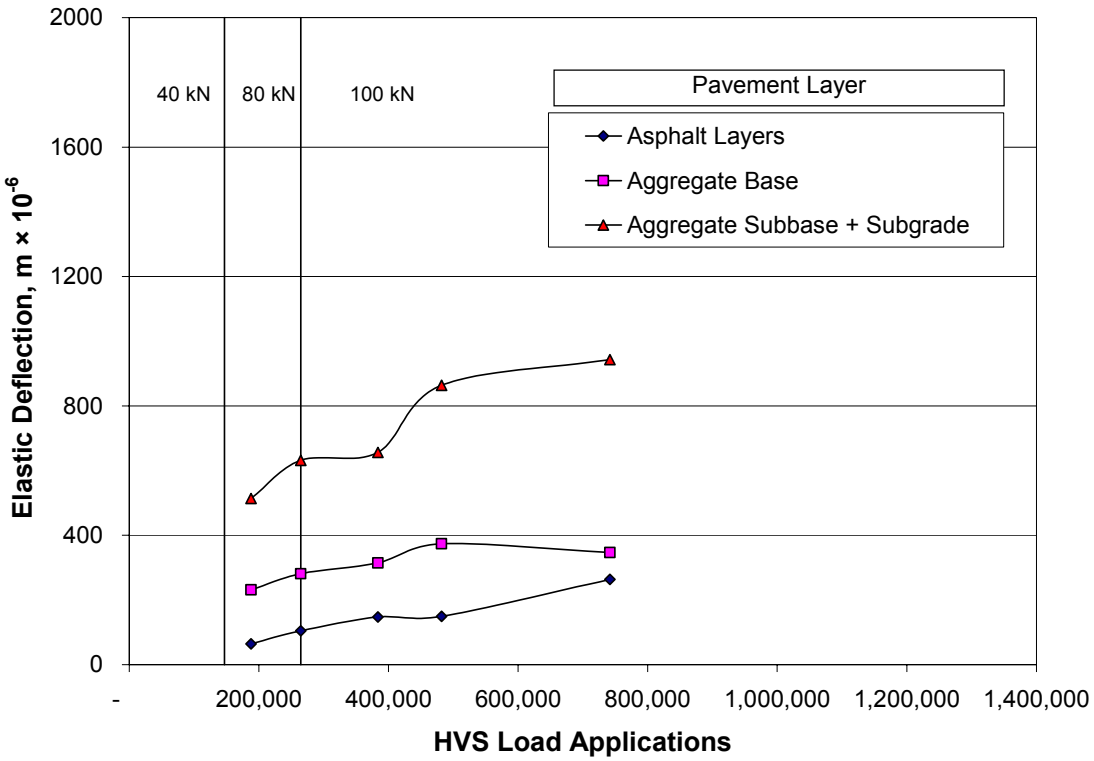

Figure 19. Layer elastic deflections resulting from 80-kN test load.

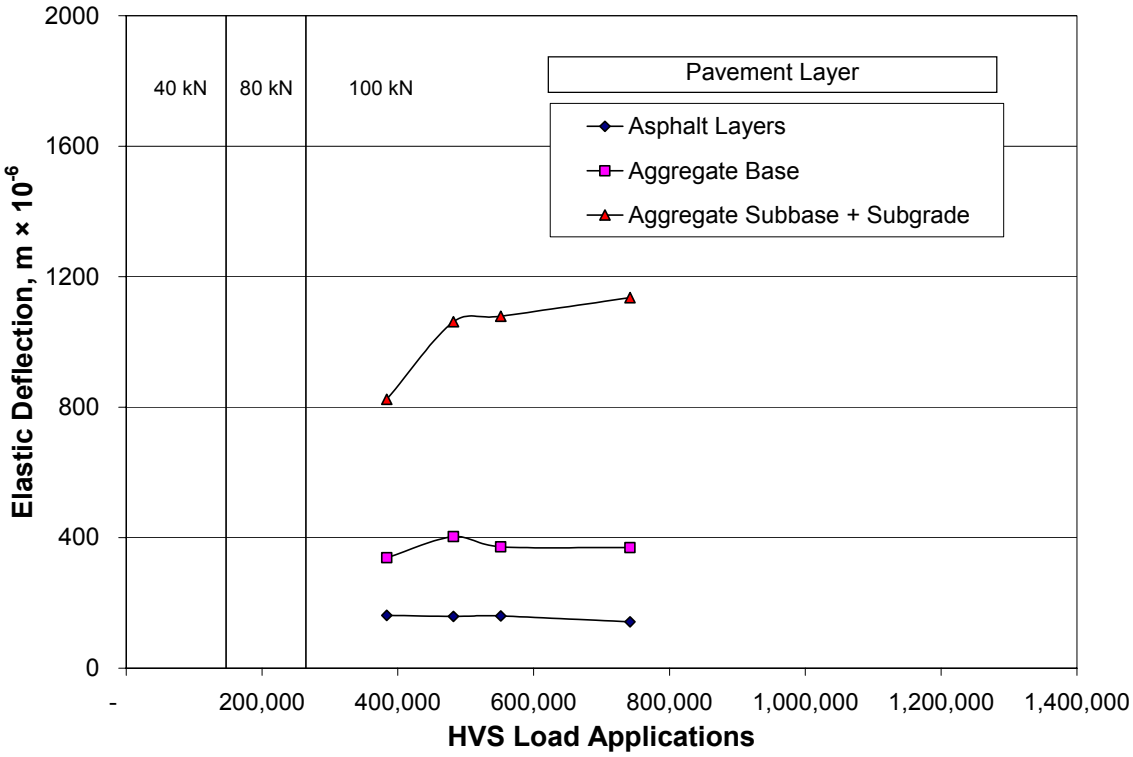

Figure 20. Layer elastic deflections resulting from 100-kN test load.

3.3.3 Comparison of Performance with That of Section 544

Figure 21 summarizes in-depth elastic deflections obtained under the 40-kN test load for Sections 544 and 545. The dashed lines represent in-depth data for Section 545 while the solid lines represent data for Section 544. Initially, in-depth elastic deflections were slightly higher for Section 545 than for Section 544. Thereafter, deflections increases at a faster rate with load applications for Section 545 in both the aggregate base and aggregate subbase/subgrade. Based on these results, one can conclude that the unbound layers in the two sections performed in a somewhat different manner. Such differences are likely due to differences in degree of compaction and moisture content between the unbound layers in these two sections.

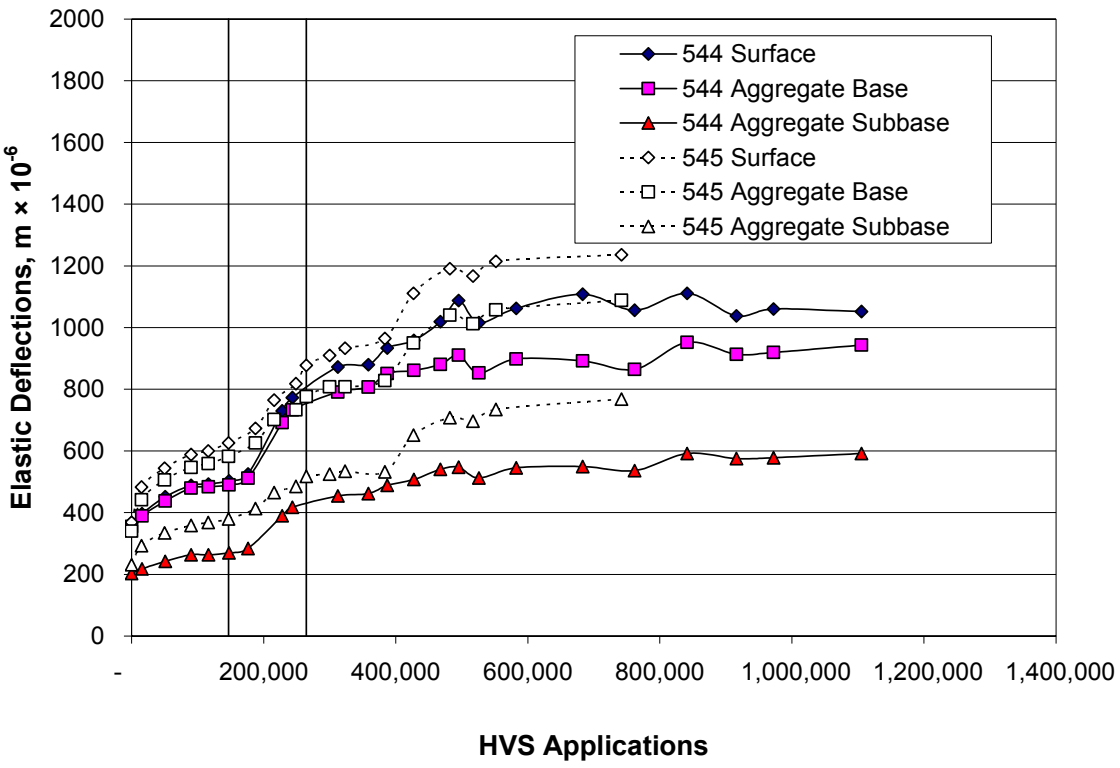

Figure 21. Comparative performance of Sections 545 and 544, elastic deflections versus HVS load applications; 40-kN test load.

3.3.4 Back-calculated Moduli from In-depth Elastic Deflections

Moduli of the pavement layers were back-calculated from the in-depth elastic deflections measured with the MDDs. Calculated deflections for the same positions were determined using the Odemark-Boussinesq method for a four-layer system (asphalt-bound layers, aggregate base layer, aggregate subbase, and subgrade). A non-linear subgrade was assumed. The error (difference of the square of the measured and calculated deflections) was minimized by changing the modulus of the layers).

Figure 22 summarizes the back-calculated moduli from the MDD data obtained for the 80- and 100-kN test load. Back-calculated moduli for the 40-kN test load yielded spurious results and have not been included. As shown in Figure 22, the modulus of the asphalt-bound layers with decreases from about 2000 MPa to 800 MPa over the course of HVS trafficking. The reduction is likely due to fatigue cracking as evidenced by the cracks present on the pavement (discussed in Section 3.4). As discussed earlier, significant damage occurred in the asphalt concrete under the 80- and 100-kN test loads. For the untreated layers, the back-calculated moduli of the aggregate subbase were slightly higher than those of the aggregate base and subgrade. The low moduli in the untreated aggregate base likely resulted from increase in the moisture content. For the subgrade, back-calculated moduli exhibited little variation throughout the applications of the 100-kN load. It will be noted that the moduli of the subgrade were similar to those of the aggregate base. These values likely result from the complex stress states as well as the nonlinear response characteristics of the untreated materials.

Figure 23 shows the back-calculated moduli for the pavement layers of Section 544. Comparisons of moduli for Sections 545 (Figure 22) and 544 (Figure 23) indicate some differences in layer moduli. The moduli for the asphalt-bound layers were lower in Section 544 than in Section 545 due in large measure to the thinner (51 mm) and less stiff asphalt rubber hot

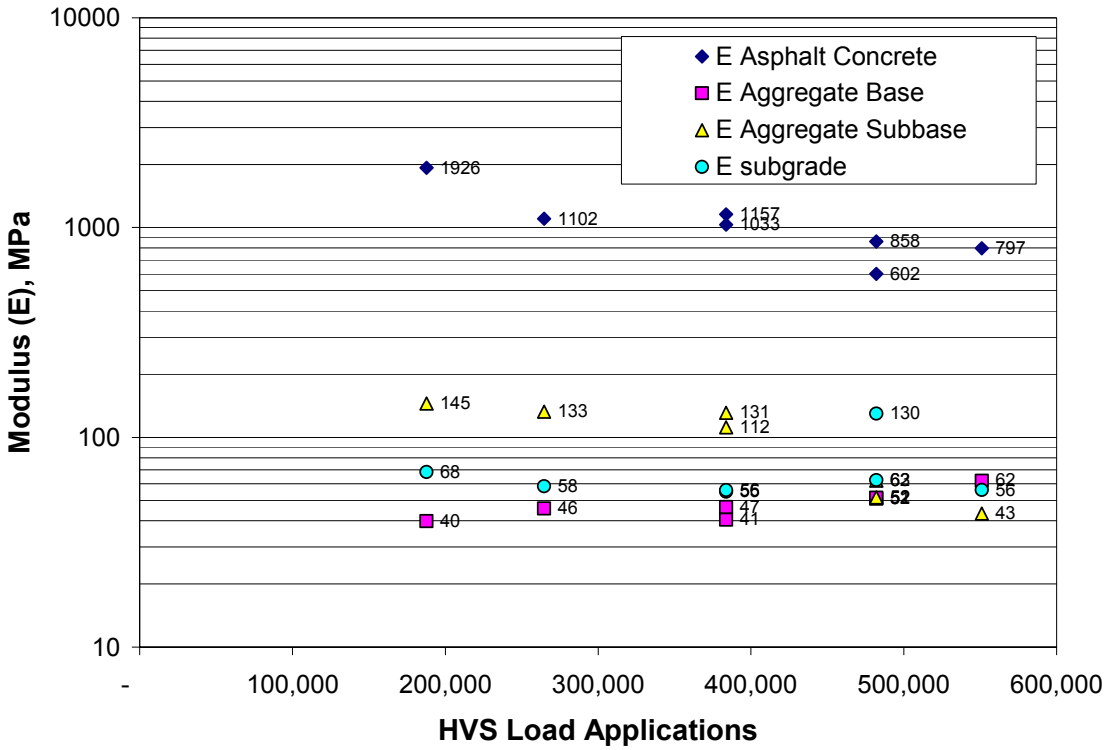

Figure 22. Layer moduli back-calculated from MDD deflections for Section 545.

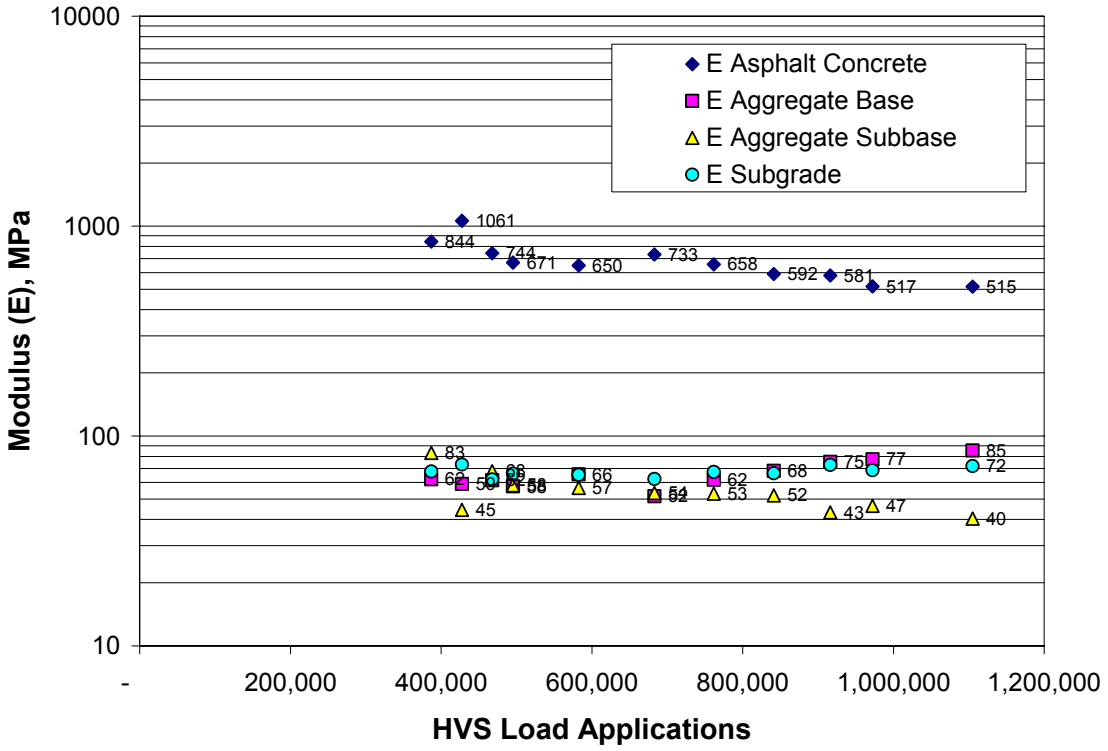

Figure 23. Layer moduli back-calculated from MDD deflections for Section 544.

mix surface layer. Moduli of the aggregate base in Section 545 were somewhat lower than those for Section 544 while the moduli of the aggregate subbase for Section 545 were larger than those for the Section 544 subbase. These may results from differences in compaction and moisture content in the unbound layers of the two sections. It will be noted that the subgrade moduli were about the same for both sections.

3.4 Crack Length Progression

Figure 24 shows cracks detected during HVS trafficking after 517,000 and 728,000 load applications. The observed cracks were predominantly transverse hairline cracks and were sometimes difficult to detect visually. The widest crack widths were approximately 0.2 mm. These hairline cracks did not spall or increase significantly in width during HVS trafficking. Lack of crack deterioration is attributed to the protected environment of the test section and to lack of fines intruding into the cracks.

Variation in the severity of cracking along the test section at the completion of the HVS trafficking is shown in Figure 25. The largest intensity of cracking occurred in the vicinity of Station 6 (200 cm along the test section).

Figure 26 shows increase of surface crack accumulation with load applications for both Sections 544 and 545. The first cracks appeared at about the same level of trafficking (500,000 load applications) even though Section 544 had a thinner wearing course than Section 545. By the time the first cracks appeared, surface elastic deflections leveled off in Section 544 but continued to increase at a slower rate in Section 545. In Section 544 [as noted in Reference (*3*)], the leveling off in deflections occurred soon after the 100-kN loading started, suggesting that crack propagation had started. In Section 545 (with the thicker asphalt concrete surface layer) while crack propagation was occurring, the crack density at the surface was not as high as that

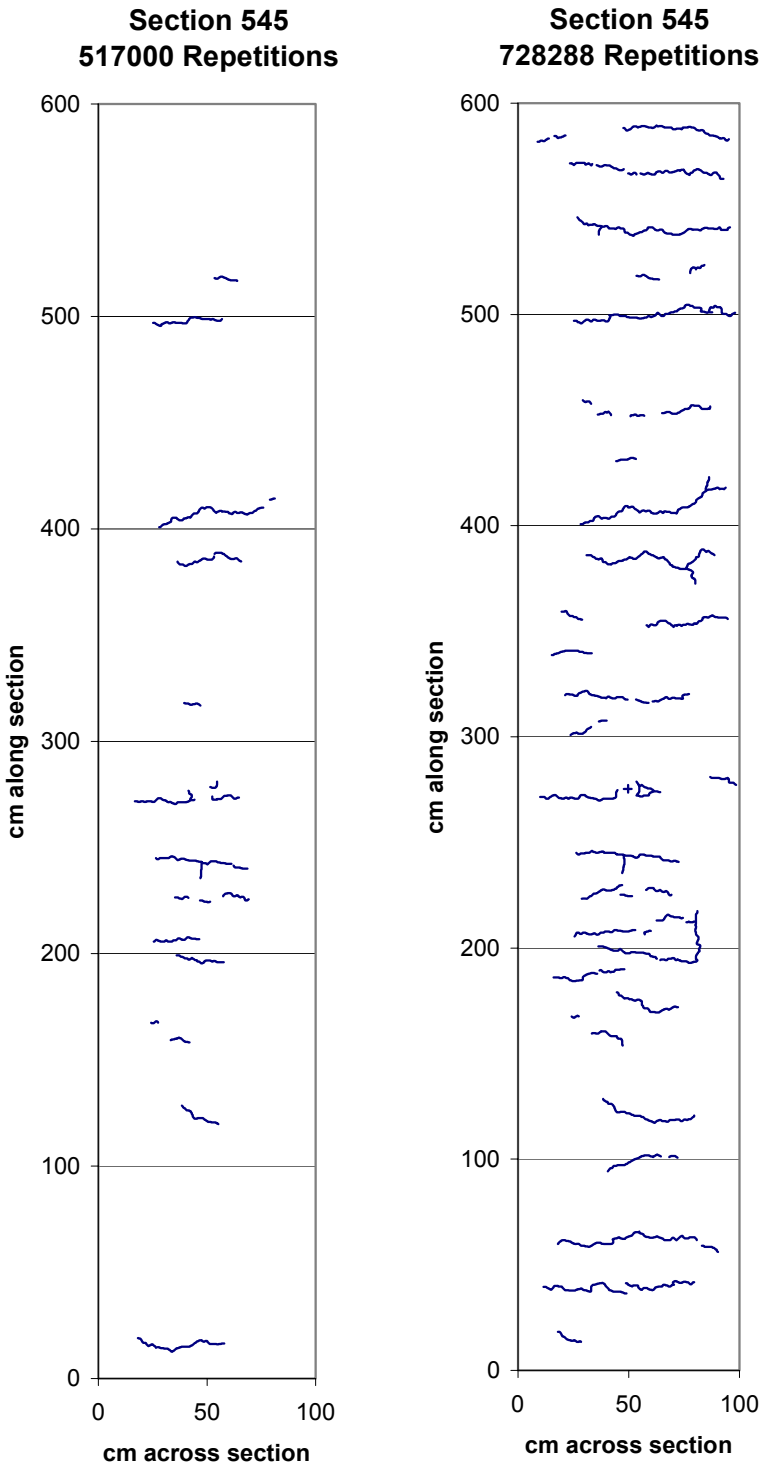

Figure 24. Surface crack schematics for Section 545.

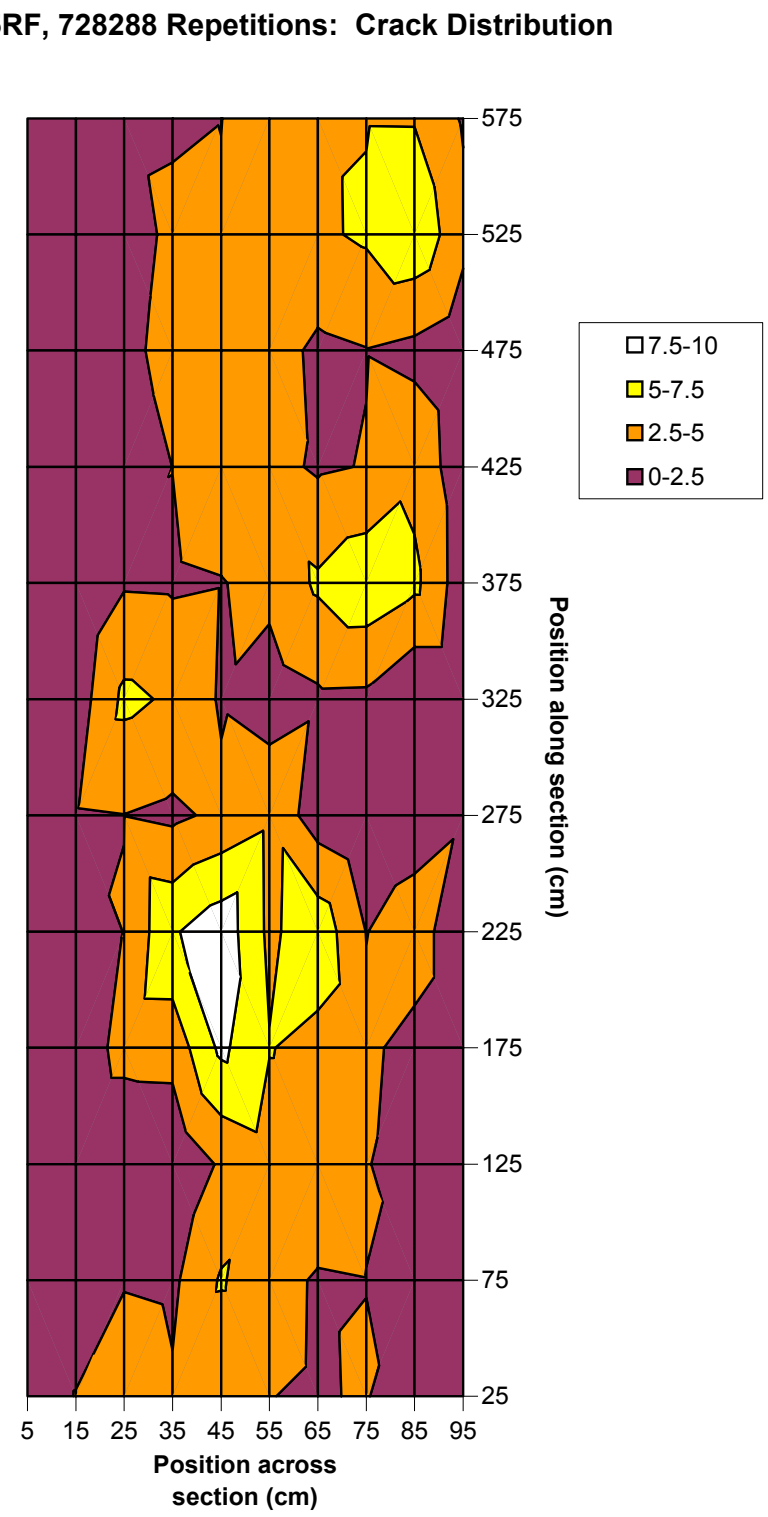

Figure 25. Contour plot of cracking density on Section 545 at the completion of HVS trafficking.

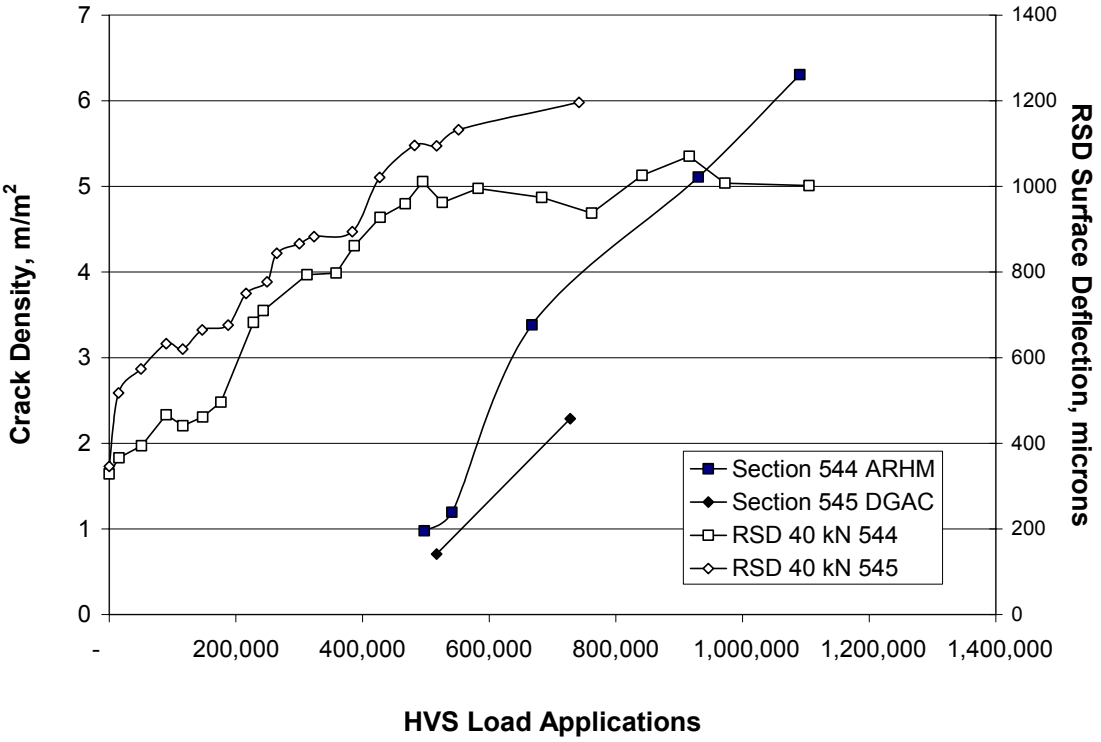

Figure 26. Comparison of crack length progression in Sections 545 and 544 together with corresponding RSD measured deflections as a function of HVS load repetitions.

observed in Section 544, indicating comparatively less damage at approximately 730,000 repetitions. Had trafficking continued, deflections in Section 545 would have reached a constant value with a crack density similar to that exhibited in Section 544.

3.5 Falling Weight Deflectometer (FWD) Testing

FWD testing was conducted on Section 545 to evaluate the structural integrity of the pavement and to estimate moduli of the layers from the measured deflections. FWD testing was conducted along the centerline of the pavement at 1-foot intervals. Three load levels (20, 40, and 60 kN) were applied to assess non-linearities in the pavement response. Loads were applied to

the pavement by a 300-mm diameter plate. FWD data were collected during Stages 1, 2, and 4 (FWD data was not collected during Stage 3 because the FWD does not fit beneath the HVS).

3.5.1 FWD Normalized Deflections

Figure 27 summarizes FWD elastic deflections measured under the load plate. These deflections have been moralized to a 40-kN load (termed D_0) for the three test stages during which the FWD testing was conducted. The figure shows that D_1 deflections showed no significant variation in D_0 deflections occurred between Stage 1 (no water infiltration) and Stage 2 (water infiltration). However, a significant increase in deflections was observed during Stage 4. Table 7 summarizes average normalized deflections obtained during the three periods of FWD testing. It will be noted that in Stage 4 (after HVS testing), deflections were more than three times those measured during Stages 1 and 2.

Table 7 Normalized Deflections (D_0) in Section 545.

Stage	Test Date	Average Deflections, m × 10^{-6}	Standard Deviation, m × 10^{-6}	Average Temperature, ºC
1	May '99	126.2	6.0	25.8
2	July'99	127.5	11.5	19.0
	Aug'99	132.6	11.7	19.8
	Sept'99	136.8	13.8	20.2
	Oct'99	138.4	14.5	22.0
	Nov'99	130.1	14.0	18.8
	Feb'00	116.9	8.8	12.5
	Mar'00	119.2	7.1	18.0
	June'00	142.9	9.2	23.0
	Oct'00	129.9	8.7	18.0
	Oct'00	137.8	11.0	16.0
4	July'01	446.4	34.7	20.0

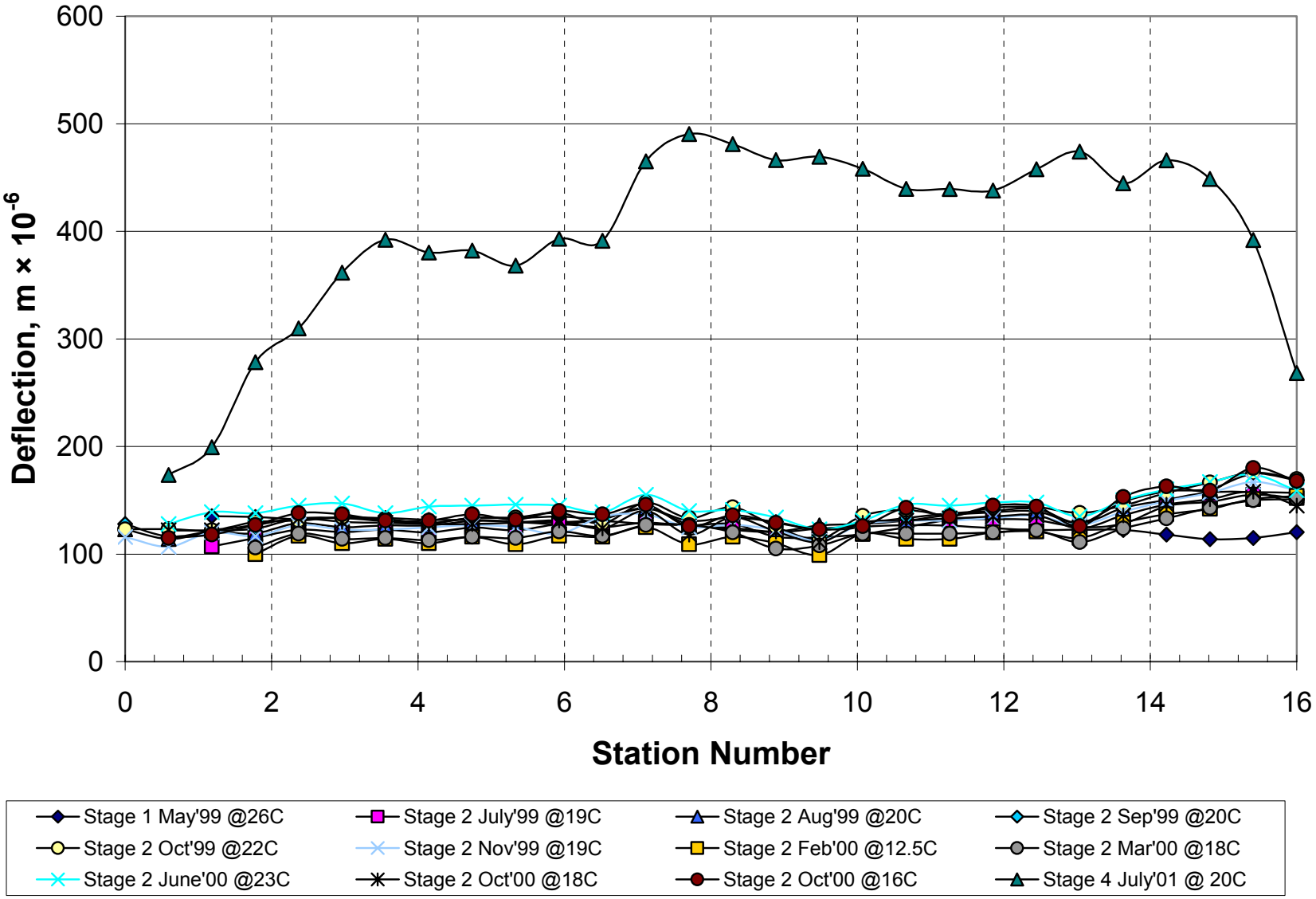

Figure 27. FWD deflections normalized to a 40-kN load for Stages 1, 2, and 4.

3.5.2 Back-calculated Moduli from FWD Deflections

Moduli were back-calculated from FWD deflections obtained from the three target loads for a three-layer system: asphalt-bound layers (AC), aggregate base layers (AB), and the subgrade (SG). A three-layer system was selected for simplicity. The back-calculation process was conducted using the program ELMOD 4.5, which uses the Odemark-Boussinesq method and assumes a nonlinear subgrade. Table 8 summarizes the layers and thicknesses for the two cases considered.

Table 8 Summary of Layers and Thicknesses Considered for Back-calculation

Layer	Thickness, mm
AC (asphalt-bound layers)	233
AB (aggregate base and aggregate subbase)	504
SG (subgrade)	assumed infinite

Results of the back-calculation process are presented in Figures 28 through 30. Results are presented for the three load levels used during FWD testing. Also presented in the figures are results of the back-calculation process using the MDD deflections (Stage 3) for the 80- and 100-kN dual wheel load.

Moduli of the asphalt concrete layers are shown in Figure 28. Moduli of the combined asphalt concrete layers ranged from 6,000 to 10,000 MPa and variations follow estimated pavement temperatures. Pavement temperatures were estimated from air temperatures using the BELLS equation. Asphalt concrete moduli after HVS testing were about 25 percent of the moduli before HVS testing. Reduction in the asphalt concrete modulus reflects fatigue damage produced by the HVS trafficking.

Moduli of the aggregate base layers are shown in Figure 29. During Stage 2, moduli ranged from 250 to 350 MPa under the three load levels. Generally, all three load levels yielded

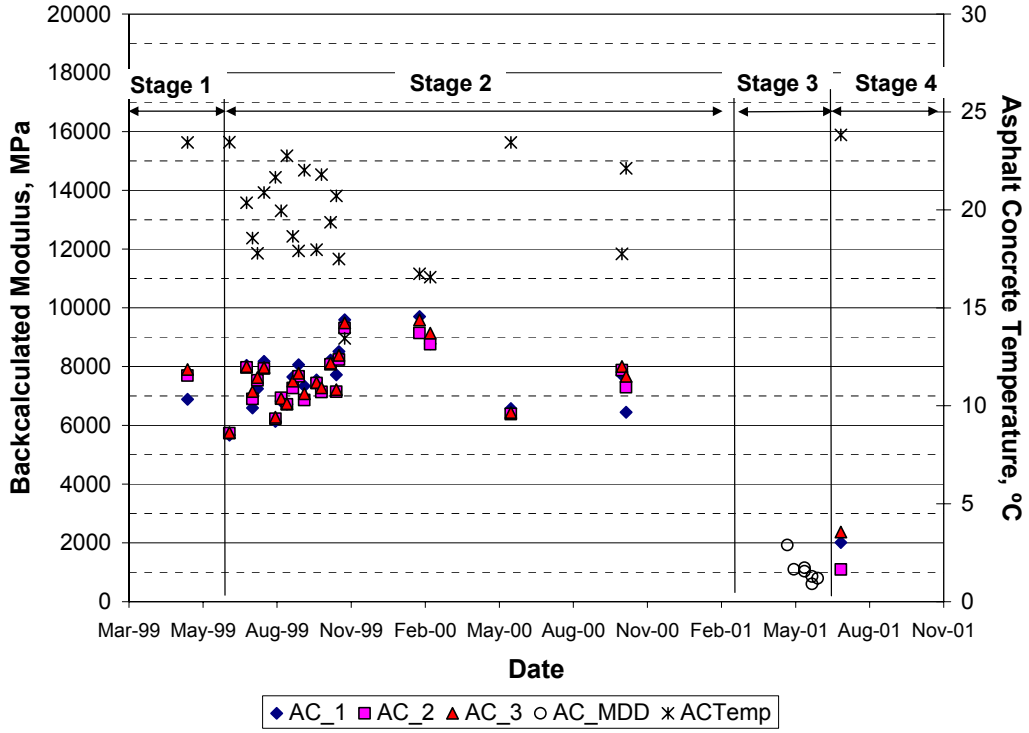

Figure 28. Back-calculated asphalt concrete moduli.

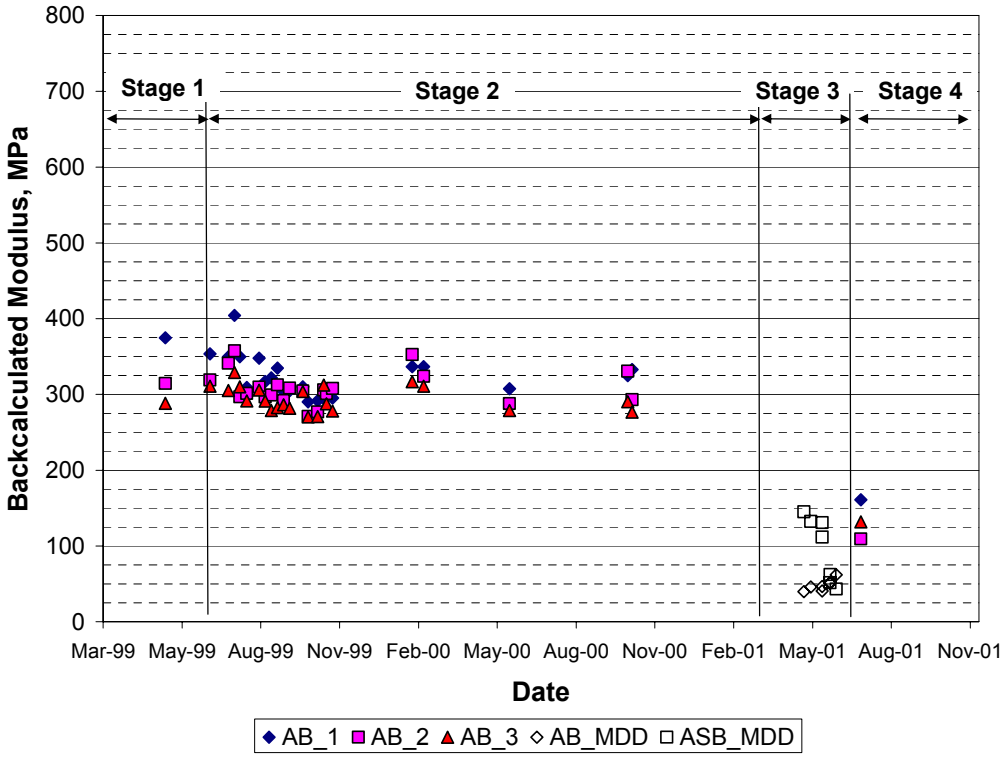

Figure 29. Back-calculated aggregate base/subbase moduli.

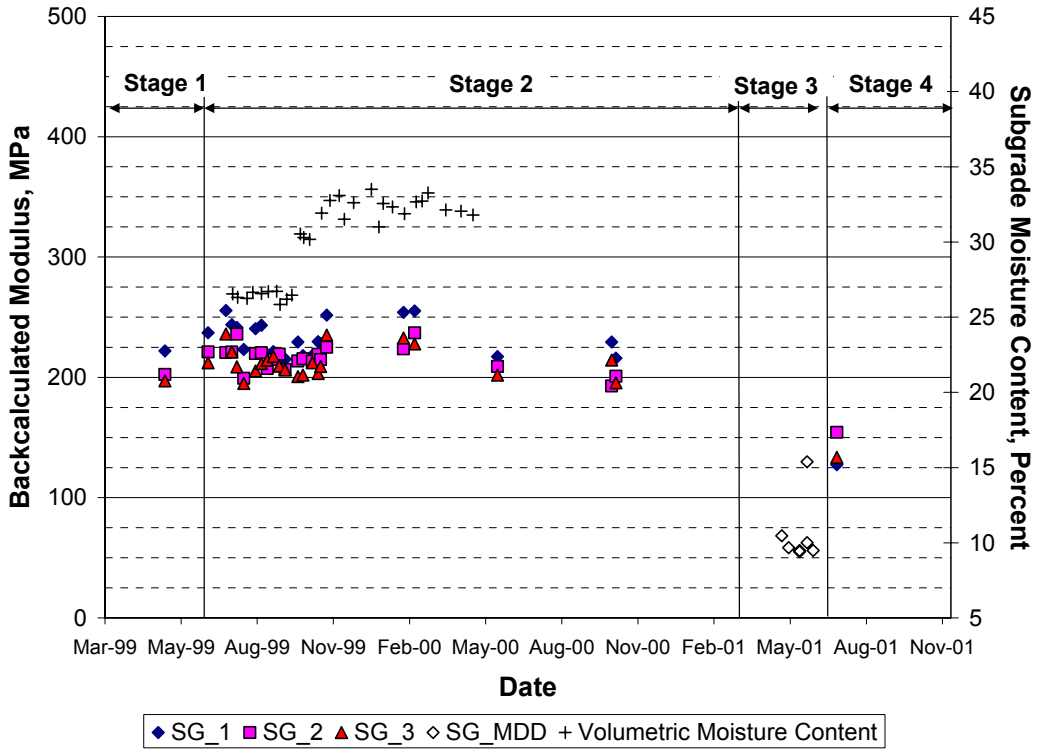

Figure 30. Back-calculated subgrade moduli.

similar values for the modulus. Aggregate base moduli after HVS trafficking dropped to values between 100 and 175 MPa. The reduction is likely due to an increase in moisture content caused by the infiltrated water, and by a change in stress state resulting from asphalt concrete damage.

Moduli and volumetric moisture contents of the subgrade layer are shown in Figure 30 for the four stages of testing. Subgrade moduli ranged from 200 to 260 MPa before testing with higher modulus associated with higher load. The subgrade modulus dropped down to 125-150 MPa after HVS testing.

Back-calculated moduli from in-depth MDD deflections (Stage 3) are also presented in the figures for comparison with the FWD results at the end of HVS testing (Stage 4). Back-calculated moduli using both methods were similar for the asphalt concrete and aggregate base layers. Moduli of the asphalt concrete back-calculated from MDD deflections were lower than

those back-calculated from FWD deflections. The results were expected since the rate of load application was lower under the MDD than for FWD testing.

Back-calculated moduli for the subgrade using the MDDs were about 50 percent of those obtained from calculations. This difference is likely related to the method used to estimate moduli from the MDD deflection data. Since the MDD at the subgrade level was not working, the back-calculation process did not include these data but adjusted the modulus of the subgrade based on the deflection data of the upper layers. Nevertheless, back-calculated subgrade moduli obtained for Sections 545 and 544 yielded similar values to those shown in Figure 30. Differences in the moduli of the subgrade back-calculated from MDD and FWD deflections are probably due to other factors such as rate of loading effects and stress state differences.

3.6 Forensic Activities

Forensic activities included core extraction, dynamic cone penetrometer testing, and trenching of the test section for direct observation of deformations in the pavement structure. Figure 31 shows a layout of the locations where forensic information was obtained.

3.6.1 Air-Void Contents from Extracted Cores

Figure 32 summarizes air-void content data for all the bound layers. No significant reductions in air-void content were observed along the centerline of the test section.

Table 9 summarizes average air-void contents in the bound layers along three distinct regions of the test section: 1) centerline; 2) “hump areas,” which are the zones of uplifted material at the edges of the trafficked area; and 3) non-trafficked areas (see Figure 31 for locations).

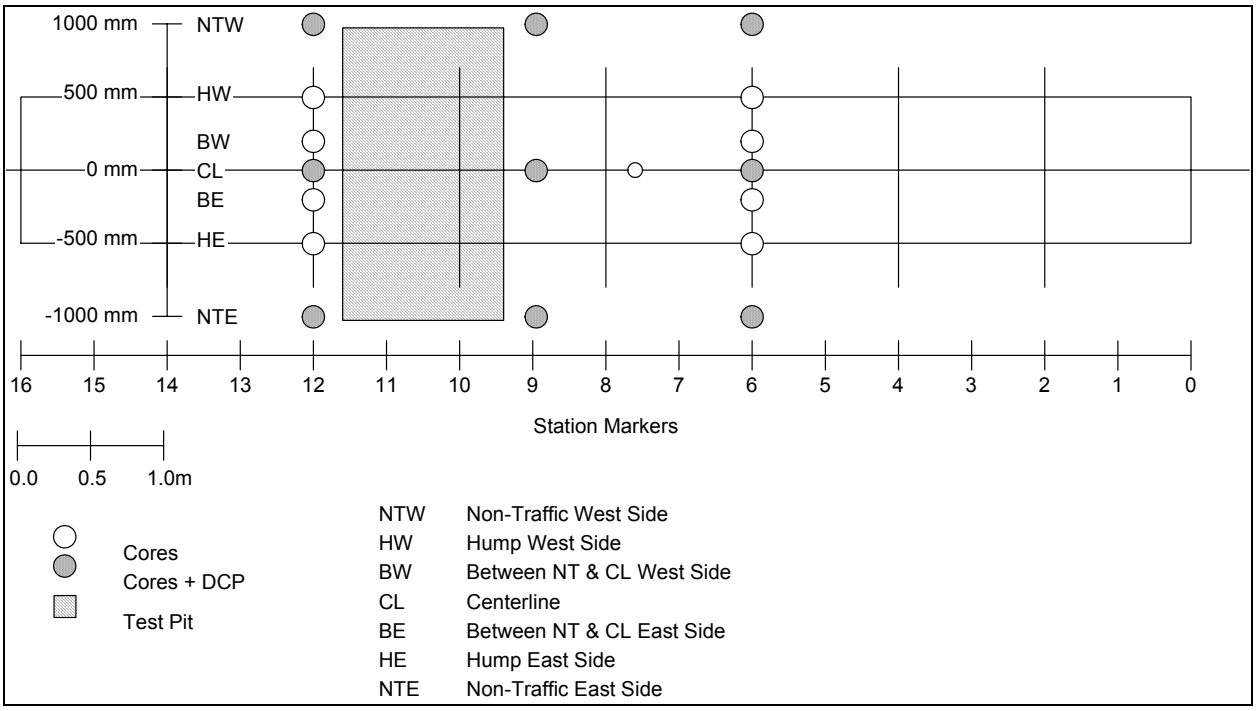

Figure 31 Layout of forensic measurements for Section 545.

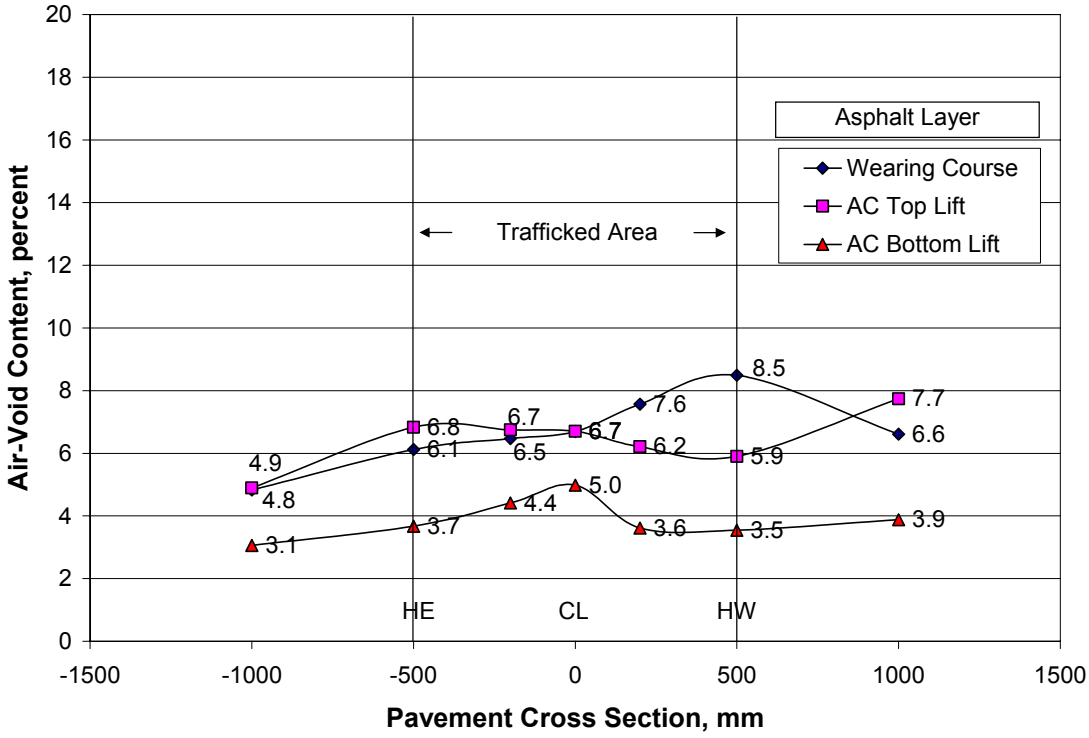

Figure 32. Average air-void contents across Section 545.

3.6.2 Bonding Between Layers

The degree of bonding between asphalt layers is an important contributor to the performance of an asphalt concrete layer. A strong bond between the layers will provide a longer pavement life. At the conclusion of HVS loading, Section 545 exhibited no bond between the asphalt layers in the trafficked areas, including the overlay and the existing pavement. This differs from the results of the Goal 3 test in a similar section. It is conjectured that the higher deflections in this test under the 80- and 100-kN loads resulting from the weakened base contributed to this debonding, even though a tack coat had been applied at the time of construction of the overlay.

Table 9 Summary of Air-Void Contents for Section 545

Asphalt Layers	Air-Void Content in Region, Percent		
	Trafficked Area	Hump Areas	Non-Trafficked Areas
DGAC Wearing Course	6.7	7.3	5.7
Asphalt Concrete, Top Lift	6.7	6.4	6.3
Asphalt Concrete, Bottom Lift	5.0	3.6	3.5

3.6.3 Dynamic Cone Penetrometer (DCP) Data

Figures 33–35 present Dynamic Cone Penetrometer (DCP) data for Section 545 (Figure 31 shows DCP test locations). The DCP plan allows for comparison of the penetration rates of the unbound layers in the non-trafficked and trafficked areas.

Table 10 summarizes DCP penetration rates for the aggregate base, aggregate subbase, and subgrade. In general, the data indicate lower penetration rates for the aggregate subbase, followed by the aggregate base, and the subgrade. Lower penetration rates indicate higher resistance to shear. Accordingly, the aggregate subbase would be expected to have higher resistance to shear than the aggregate base. For the aggregate base, somewhat lower penetration

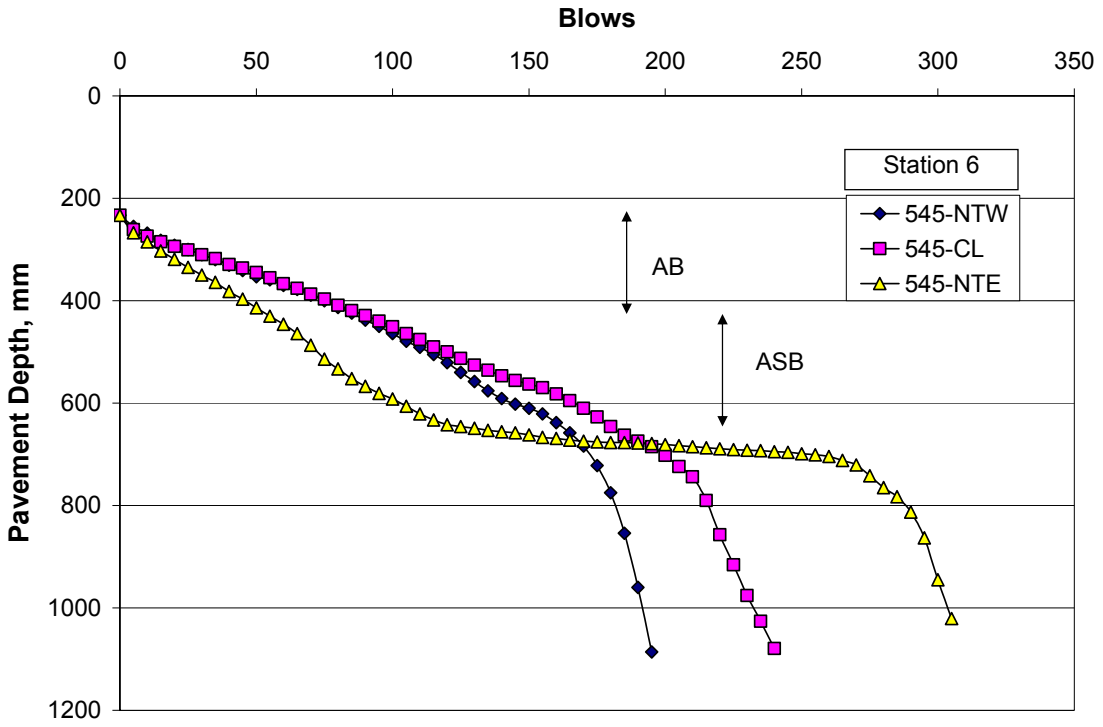

Figure 33. DCP results for Section 545, Station 6.

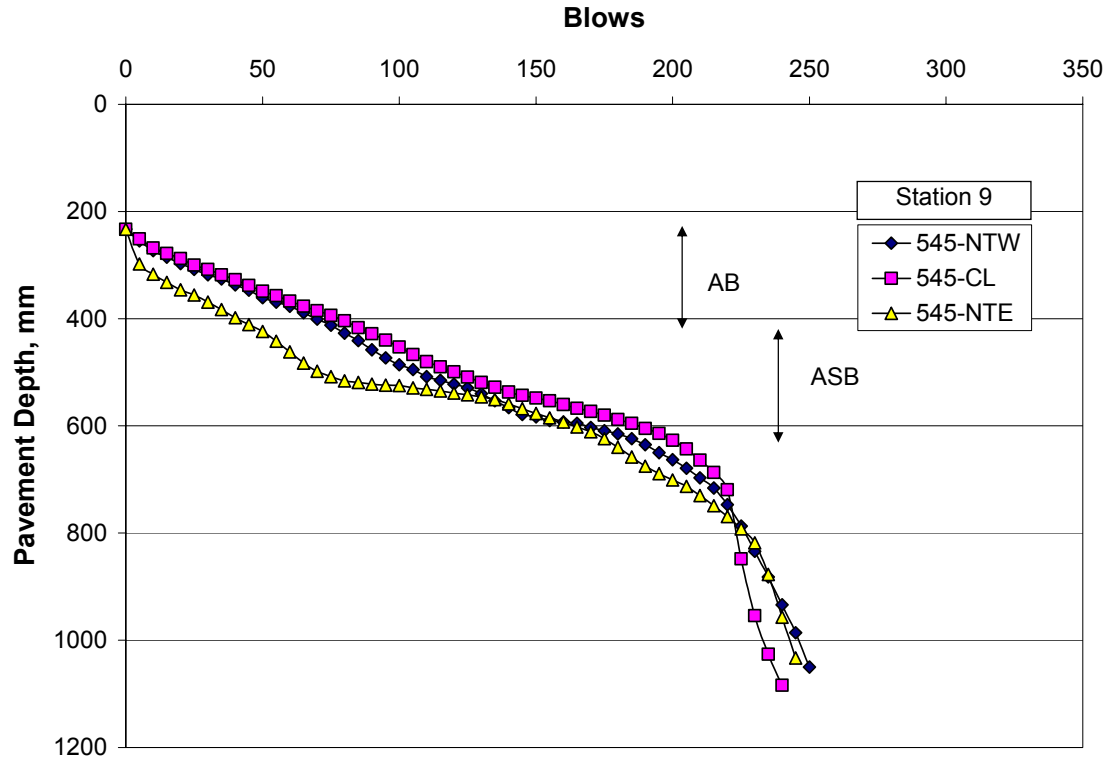

Figure 34. DCP results for Section 545, Station 9.

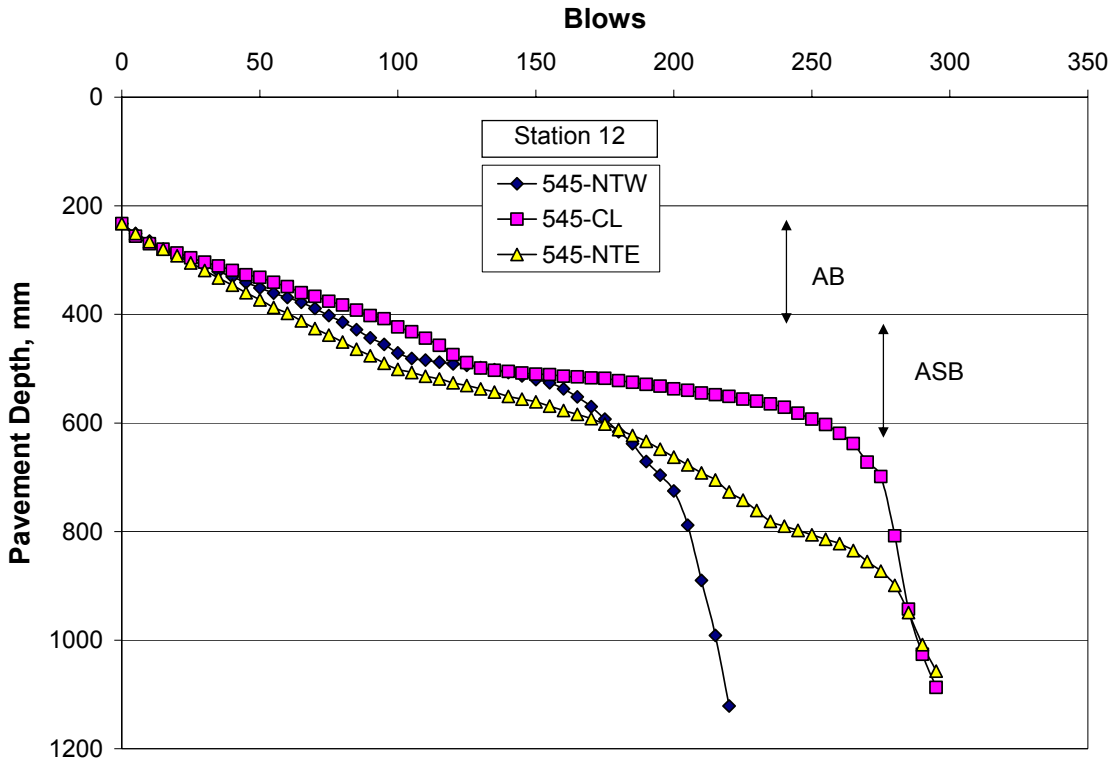

Figure 35. DCP results for Section 545, Station 12.

Table 10 Summary of DCP Penetration Rates

DCP Test Location*		Penetration Rate (mm/blow count)		
		Aggregate Base	Aggregate Subbase	Subgrade
Station 6	NTW	2.2	2.4	20.8
	CL	2.0	3.2	9.4
	NTE	3.5	0.6	12.7
Station 9	NTW	2.3	1.1	10.4
	CL	2.1	1.4	18.2
	NTE	3.0	1.9	14.5
Station 12	NTW	2.1	1.0	19.9
	CL	1.8	0.6	19.9
	NTE	2.6	1.8	10.7
Average	NTW	2.2	1.5	17.0
	CL	2.0	1.7	15.8
	NTE	3.0	1.4	12.6

*Refer to Figure 23 for explanation of test locations.

rates were obtained for the centerline than in the non-trafficked areas; this difference can be attributed to increased density produced by HVS trafficking.

The result of DCP tests in the subbase as compared to those for the base are in line with the modulus values calculated from the MDD deflections (Figure 22).

3.6.4 Trench Data

After the completion of HVS trafficking, a transverse test pit was excavated in order to enable direct observation of the pavement layers. Measurements from the trench were used to estimate thickness and rutting in the pavement layers. Figures 36 and 37 show profile data at the interface of each layer at the completion of HVS trafficking. During the data collection process, it was difficult to establish the boundary between the asphalt concrete and the aggregate base due to roughness at the interface of the two layers. The profiles show that the subbase thickness varied considerably across the section. Differences in subbase thickness were anticipated and reported in previous CAL/APT reports (*4–8*).

Table 11 summarizes average layer thicknesses at various locations across the both faces of the test pit; the results are plotted in Figure 38.

Table 11 Comparison of Layer Thicknesses across Section 545

Location*	Thickness (mm) of Pavement Layer									
	DGAC Wearing Course		DGAC Lift 1		DGAC Lift 2		Aggregate Base		Aggregate Subbase	
	St. 9	St. 12	St. 9	St. 12	St. 9	St. 12	St. 9	St. 12	St. 9	St. 12
NT-W	90	87	60	62	86	84	260	258	204	209
H-W	92	91	59	61	87	84	249	260	218	213
B-W	91	91	59	60	83	83	251	252	229	236
CL	90	88	60	60	83	82	240	258	249	260
B-E	91	90	61	61	82	79	252	260	247	271
H-E	92	91	61	62	81	80	271	255	262	295
NT-E	90	90	63	62	77	79	260	260	260	300

*Refer to Figure 31 for explanation of pavement locations.

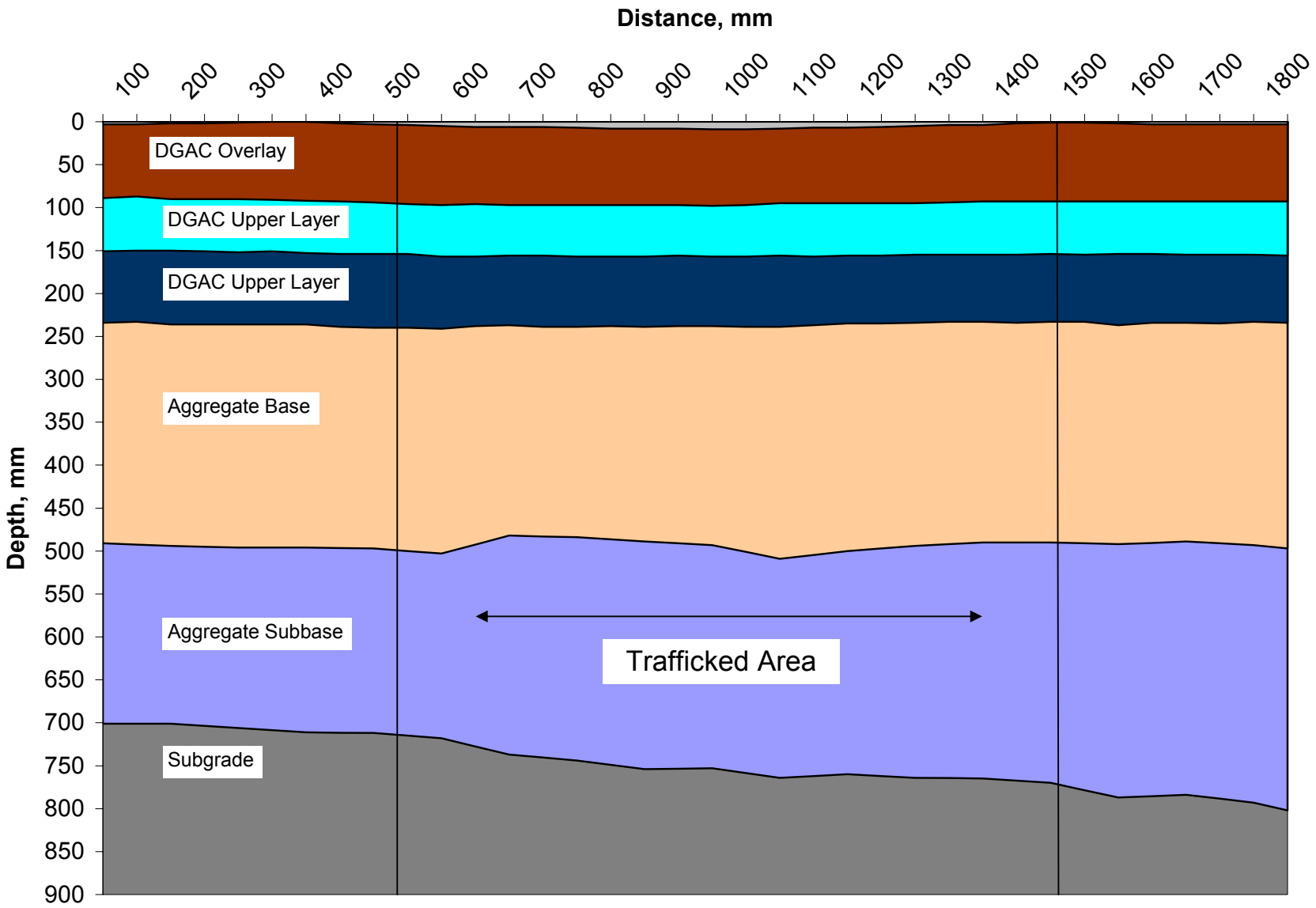

Figure 36. Trench data, south face of trench at Station 12, Section 545.

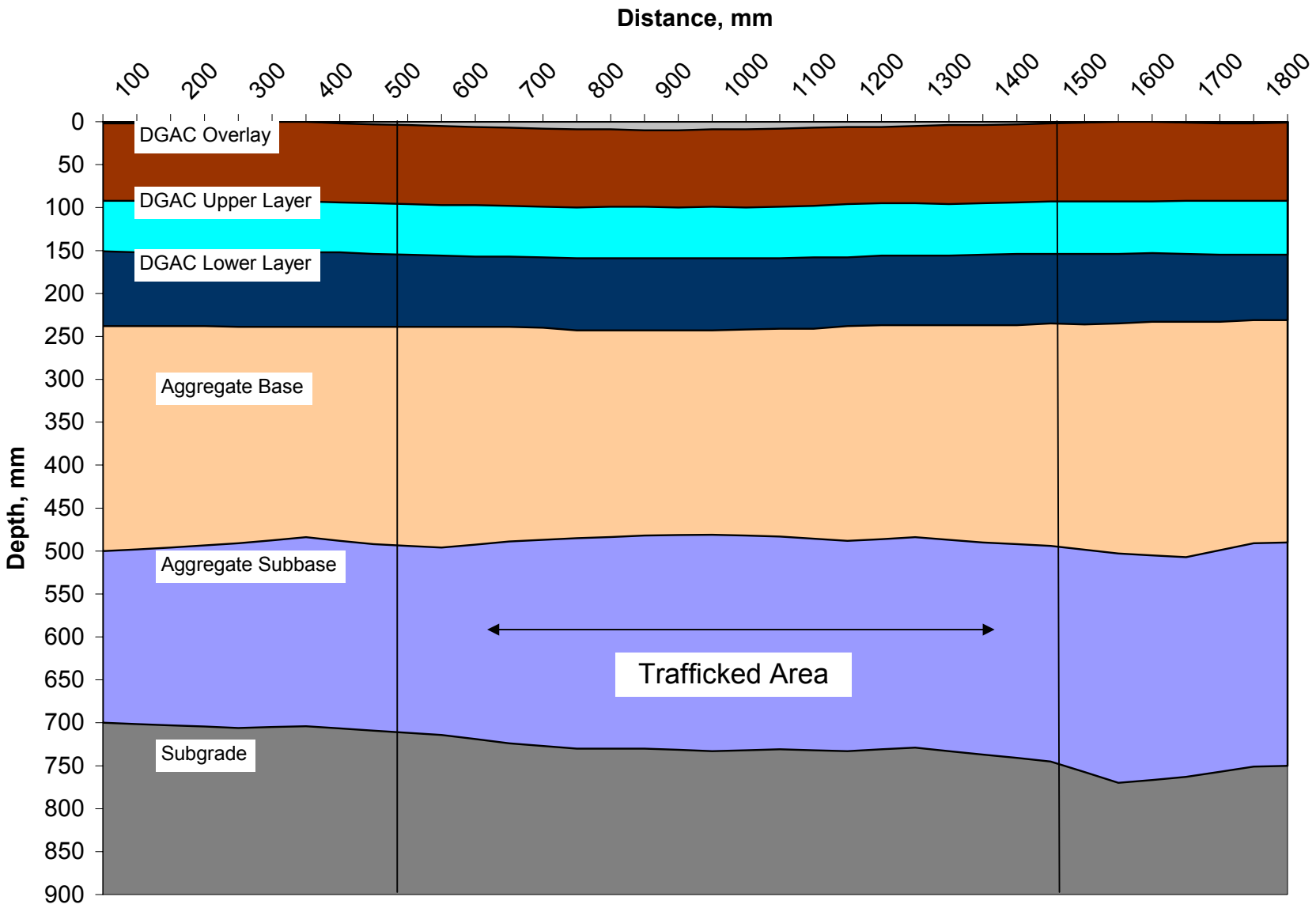

Figure 37. Trench data, north face of trench at Station 9, Section 545.

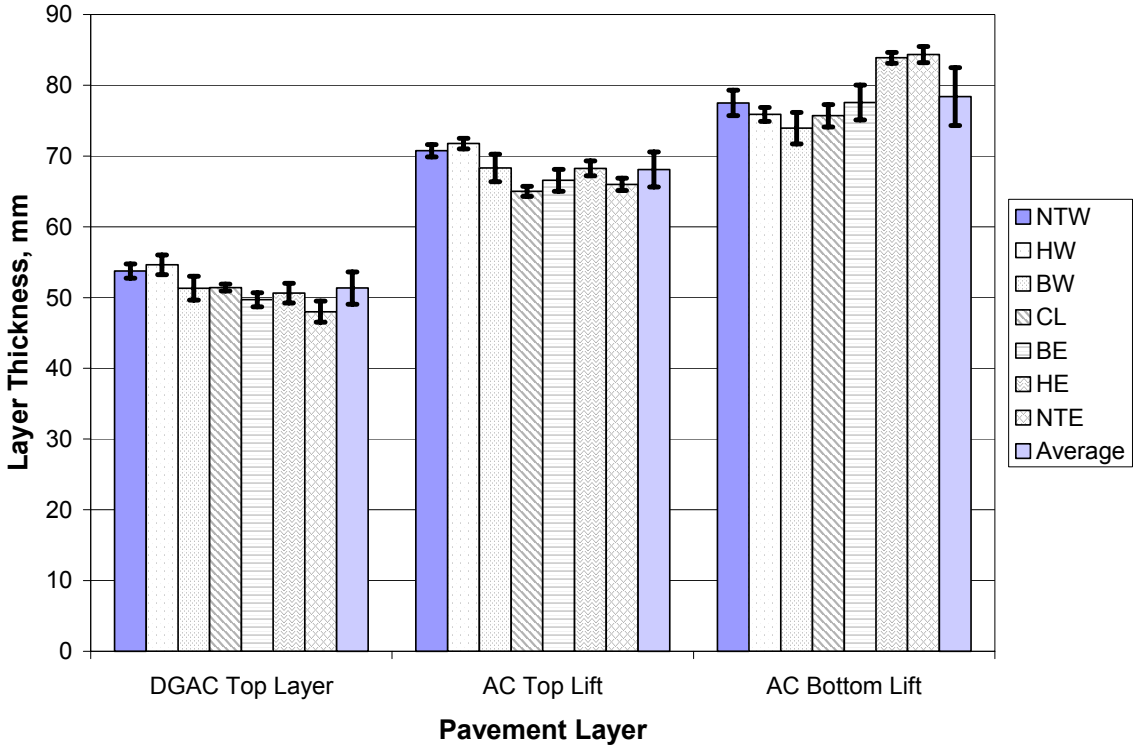

Figure 38a. Asphalt-bound layers.

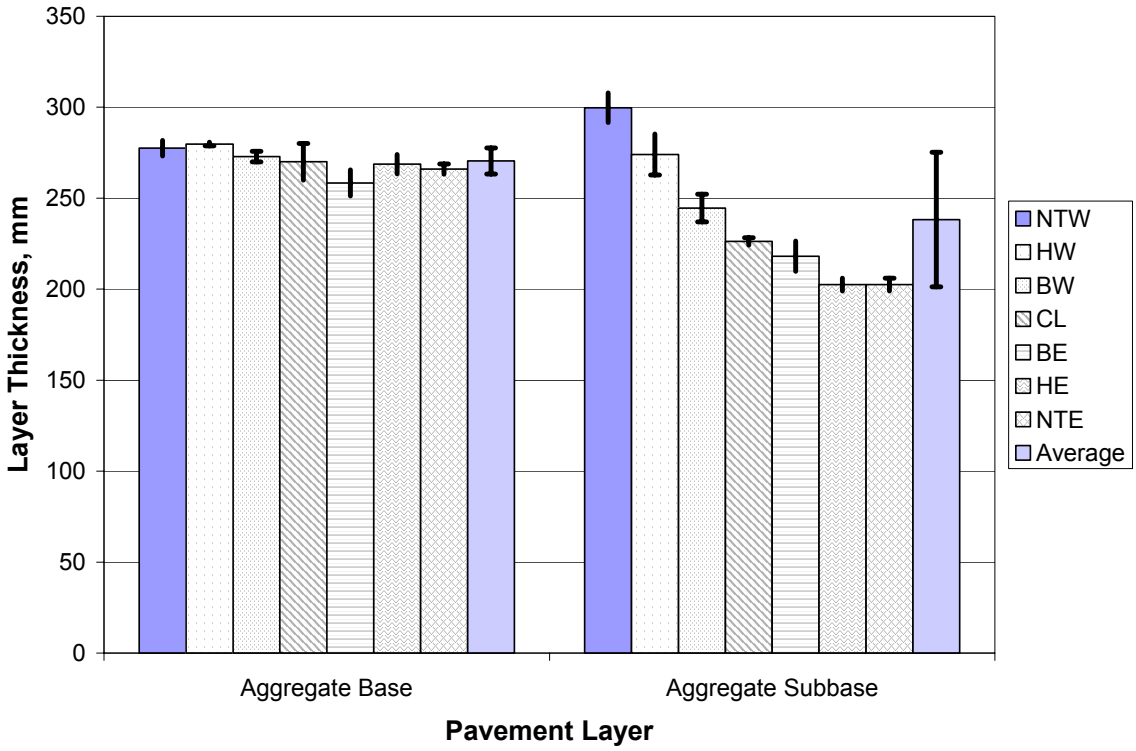

Figure 38b. Untreated aggregate layers.

Figure 38. Measured layer thicknesses in test pit.

With this variability occurring before trafficking, it was difficult to establish the level of rutting of the individual layers. In addition, measurement variability and roughness at the layer interfaces made it difficult to determine the level of rutting in each individual layer from the thickness measurements, particularly in the unbound layers.

Based on the information provided by the MDDs and air-void content data, little rutting occurred in the DGAC layer since no significant variation in air-void content was observed. Based on the MDD data, a total of 2 mm of rutting was measured for the asphalt concrete layers. Due to variability in asphalt concrete thickness in the test pit, the MDD measurements could not be verified. From the same MDD data, 7 mm of rutting was measured in the aggregate base. This also could not be verified using the test pit data.

4.0 PERFORMANCE EVALUATION AND MECHANISTIC ANALYSIS

At the end of HVS testing, Section 545 was subjected to 147,000 applications of the 40-kN load, 117,000 applications of the 80-kN load, and 477,000 applications of the 100-kN load. The number of applied loads were converted to equivalent 80-kN single axle loads (ESALs) using a load equivalency exponent of 4.2 per Caltrans procedures, which results in a total of 21.3 million ESALs. The number of ESALs to failure as defined in the test program for surface rutting (12.5 mm) and cracking (2.5 m/m^2) were 73.3 and 21.3 million, respectively. Like Section 544, Section 545 failed by fatigue cracking. The rutting failure level was not reached during testing, thus the 37.3 million ESALs is only an estimate.

Results of this test provided the opportunity to compare the performance of the 90-mm DGAC overlay with the 50-mm ARHM-GG overlay of Section 544 under saturated base conditions. Failure in fatigue occurred at about 14.3 million ESALs for Section 544, somewhat less than the 21.3 million ESALs for Section 545.

To compare the performance of Section 544 and 545, mechanistic analyses were performed on the response of the two sections to 40- and 100-kN single wheel loads.

4.1 Pavement Responses

Pavement responses considered for analysis included the tensile strain on the underside of the asphalt concrete layer and the vertical compressive strain at the surface of the unbound layers. Table 12 summarizes the pavement thicknesses and layer moduli for the two sections. The layer moduli selected were average back-calculated moduli obtained from FWD testing.

Table 12 Summary of Pavement Structures for Analysis

Test Section	Layer	Thickness, mm	Moduli before HVS testing, MPa
544	AC	200	5900
	AB	532	338
	SG		195
545	AC	233	7480
	AB	504	308
	SG		216

Table 13 summarizes the calculated responses under 40- and 100-kN wheel loads on dual tires for the two cases considered. These responses suggest that Section 545 should perform slightly better than Section 544 as indicated by lower tensile strains and lower stresses at the surface of the aggregate base for Section 545.

Table 13 Summary of Pavement Responses under 40-kN Load

Pavement Response	Section 544		Section 545	
	40 kN	100 kN	40 kN	100 kN
Tensile Strain Bottom of AC, μstrain	67	146	45	105
Vertical Stress Top of AB, kPa	65	148	40	94
Vertical Stress Top of SG, kPa	27	58	25	54

4.2 Fatigue Analyses

The fatigue analysis and design system used in this report is presented Figure 39 and discussed in Reference (*9*).

For this particular analysis, a design reliability of 50 percent was assumed, obtaining a reliability multiplier of 1.0. The laboratory fatigue life equation for the mixes used in the simulation is:

$$\ln N = -21.9295 - 0.106663 AV - 4.14248 \ln \varepsilon \quad \textbf{(1)}$$

where:

N = the number of repetitions to failure obtained from laboratory fatigue beam tests tested under strain control,
AV = the percent air-void content of the mix, and
ε = the tensile strain at the bottom of the asphalt concrete.

The expressions for the shift factor (SF) and temperature conversion factor (TCF) utilized are:

$$SF = 3.1833 \times 10^{-5}\, \varepsilon^{-1.3759} \quad \textbf{(2)}$$

$$TCF = 1.754 \ln(d) - 2.891 \quad \textbf{(3)}$$

where:
d = thickness of the asphalt concrete layer in centimeters.

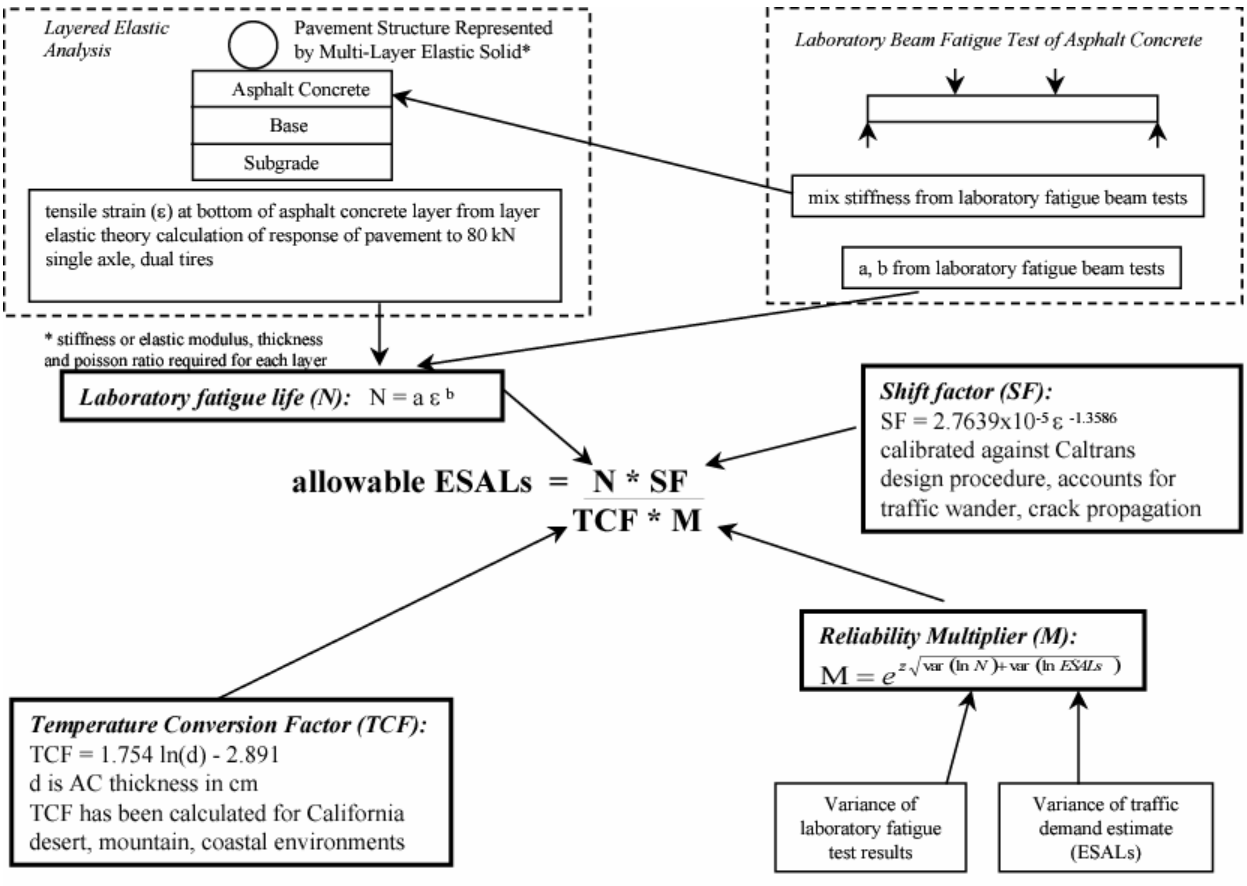

Figure 39. Methodology followed in the fatigue analysis system to determine ESALs.

The results of the simulation process are summarized in Table 14.

Table 14 Summary of Calculation of ESALs using the UCB Fatigue Analysis System

Case	μStrain	AV, %	ln N	N, millions	SF	t_{AC}, cm	TCF	M	ESALs, millions
Section 544, 40 kN	67	4.6	17.40	35.9	17.6	20.0	2.36	1	267
Section 544, 100 kN	146	4.6	14.17	1.4	6.0	20.0	2.36	1	3.6
Section 545, 40 kN	50	4.6	18.61	120.7	26.3	23.3	2.63	1	1,209
Section 545, 100kN	105	4.6	15.54	5.6	9.5	23.3	2.63	1	20.1

The results of the simulation suggest that Section 545 should have at least 4 times the fatigue life of that of Section 544. However, the HVS testing indicated that the fatigue life of Section 545 was only about 1.5 times longer than that of Section 544. This difference between the simulation and the actual performance may result from some differences in the characteristics of the materials used as well as assumptions about thicknesses and moduli of the asphalt bound layers. For example, it was assumed that the asphalt layers of both sections consisted of the same AR-4000 DGAC mix. While this is true for Section 545, the upper 50 mm of the asphalt-bound layer of Section 544 consisted of an ARHM-GG mix with somewhat different fatigue characteristics.

Thus, while the results of the simulation do not produce a one-to-one correspondence, the HVS results support the current Caltrans practice of using an overlay thickness of ARHM-GG of one-half that for a DGAC overlay, even for the saturated base conditions.

5.0 SUMMARY AND CONCLUSIONS

5.1 Summary

This report presents the results of accelerated pavement testing and associated activities of Section 545 under the Goal 5 research project. Section 545 is a flexible pavement that does not include the 75-mm layer of ATPB between the asphalt concrete and the aggregate base layers and was designated as an undrained section. This report includes the analysis for the four stages of testing considered in the Goal 5 test plan for Section 545. Results of the accelerated pavement testing provided data to measure and compare the performance of two undrained structures with ARHM-GG and DGAC wearing courses under wet conditions.

The test program for Section 545 was begun in April 2001 and was completed in August 2001. Under HVS testing, 742,000 total repetitions were applied to the section consisting of 147,000 repetitions under the 40-kN dual wheel load, 117,000 repetitions under the 80-kN load, and 477,000 repetitions under the 100-kN load. The section was trafficked under conditions of wet base which was accomplished using a water infiltration system. The wet base condition simulated precipitation for an average peak week of 51.3 mm typical of the environment of Eureka, CA.

Section 545 failed in fatigue after being subjected to 21 million ESALs (based on the Caltrans load equivalency exponent of 4.2). When tested with the untreated base in the wet condition. The performance of Section 545 (DGAC overlay) was slightly better than that of Section 544 (ARHM-GG overlay)—21 million versus 14 million ESALs to failure. This difference was most likely caused by the differences in thickness and stiffness of the two overlay materials.

Because of the increased moisture content in the untreated base, pavement deflections in Section 545 were significantly larger than those for the comparable sections tested in the dry condition. Whereas for tests with the base in the dry condition, there was no debonding of the overlay from the existing pavement, debonding was observed in the overlay in Section 545 even though a tack coat had been applied. This debonding likely occurred when the 80- and 100-kN loads were applied.

5.2 Conclusions

Results of the test on Section 545 and associated response and performance analyses suggest the following conclusions:

1. Section 545, tested in the wet base condition, failed in fatigue after being subjected to an equivalent loading of 21 million ESALs. Even though the stiffness of the base was reduced due to the increase moisture content, it was estimated that it would require an additional 16 million ESALs to reach the limiting rut depth of 13 mm.
2. While the bond between the two lifts of DGAC in the initial pavement was weak due to the lack of a tack coat (*10*), one had been applied prior to placing the DGAC overlay. In spite of this, because of the increased deflections due to the 80- and 100-kN loads, debonding was also observed between the overlay and the existing pavement. The likelihood of deflections being as large as observed in Section 545 if the existing layers had been well bonded would have been reduced considerably. Thus, even with the weakened base condition, the analyses (presented in Section 4) suggest that a substantially larger number of ESALs could have been applied. This reinforces an earlier recommendation that tack coast should be applied between all lifts in asphalt concrete construction (*11*).

3. The use of mechanistic analysis, as discussed in Section 4, provides reasonable measures of comparative performance of different pavement materials and continues to emphasize the importance of its use in the design of new and rehabilitated pavements, e.g., comparison of the performance of Sections 545 and 544.
4. Results of the FWD testing provided reasonable results for the impacts of increased moisture content in the stiffness of the untreated materials in both Sections 545 and 544. These results most definitely support the continued use of data obtained from FWD testing being conducted as a part of PPRC seasonal monitoring program.
5. FWD testing was effective in establishing the structural condition of the pavement sections during all stages of testing. Changes in the modulus of the layers due to moisture content changes and trafficking were effectively determined by the device. The slight differences in performance seem to be correlated to differences in layer moduli in the asphalt concrete and aggregate base layers.

5.3 Recommendations

1. Better compaction in the ARHM layer can greatly increase the performance of this layer.

6.0 REFERENCES

1. Harvey, J., M.O. Bejarano, A. Ali. *Test Plan for Goal 5: Performance of Drained and Undrained Flexible Pavement Structures under Wet Conditions.* Pavement Research Center, Cal/APT Program, Institute of Transportation Studies, University of California, Berkeley.

2. Harvey, J., Chong, A., Roesler, J. *Climate Regions for Mechanistic-Empirical Pavement Design in California and Expected Effects on Performance.* Draft report prepared for California Department of Transportation. Pavement Research Center, CAL/APT Program, Institute of Transportation Studies, University of California, Berkeley. June 2000.

3. Bejarano, M.O., J.T. Harvey, A. Ali, D. Mahama, D. Hung, and P. Preedonant. *Performance of Drained and Undrained Flexible Pavement Structures under Wet Conditions, Accelerated Test Data Test Section 544—Undrained.* Report prepared for the California Department of Transportation. Pavement Research Center, Institute of Transportation Studies, University of California at Berkeley. Revision December 2004.

4. Harvey, J. T., L. du Plessis, F. Long, S. Shatnawi, C. Scheffy, B-W. Tsai, I. Guada, D. Hung, N. Coetzee, M. Reimer, and C. L. Monismith. *Initial CAL/APT Program: Site Information, Test Pavement Construction, Pavement Materials Characterizations, Initial CAL/APT Test Results, and Performance Estimates.* Report prepared for the California Department of Transportation. Report No. RTA-65W485-3. Pavement Research Center, CAL/APT Program, Institute of Transportation Studies, University of California, Berkeley, June 1996, 305 pp.

5. Harvey, John T., Louw du Plessis, Fenella Long, John A. Deacon, Irwin Guada, David Hung, Clark Scheffy. *CAL/APT Program: Test Results from Accelerated Pavement Test on Pavement Structure Containing Asphalt Treated Permeable Base (ATPB) Section 500RF.* Report No. RTA-65W485-3. Report Prepared for California Department of Transportation. Pavement Research Center, CAL/APT Program, Institute of Transportation Studies, University of California, Berkeley. June 1997.

6. Harvey, J., J. Prozzi, J. Deacon, D. Hung, I. Guada, L. du Plessis, F. Long, and C. Scheffy. *CAL/APT Program: Test Results from Accelerated Pavement Test on Pavement Structure Containing Aggregate Base (AB)--Section 501RF.* Report prepared for the California Department of Transportation. Pavement Research Center, CAL/APT Program, Institute of Transportation Studies, University of California, Berkeley. Draft submitted September 1997. Final submitted April 1999.

7. Harvey, J., I. Guada, C. Scheffy, L. Louw, J Prozzi, and D. Hung. *CAL/APT Program: Test Results from Accelerated Pavement Test on Pavement Structure Containing Asphalt Treated Permeable Base--Section 502CT.* Draft report submitted to California Department of Transportation. Pavement Research Center, CAL/APT Program, Institute of Transportation Studies, University of California, Berkeley. February 1998.

8. Harvey, J., D. Hung, J. Prozzi, L. Louw, C. Scheffy, and I. Guada. *CAL/APT Program: Test Results from Accelerated Pavement Test on Pavement Structure Containing Untreated Aggregate Base--Section 503RF.* Draft report submitted to California Department of

Transportation. Pavement Research Center, CAL/APT Program, Institute of Transportation Studies, University of California, Berkeley. December 1997.

9. Manuel O. Bejarano, John T. Harvey, Abdikarim Ali, Mark Russo, David Mahama, Dave Hung, and Pitipat Preedonant. *Performance of Drained and Undrained Flexible Pavement Structures under Wet Conditions Test Data from Accelerated Pavement Test Section 543-Drained*. Draft report prepared for the California Department of Transportation. Pavement Research Center, Institute of Transportation Studies, University of California Berkeley, University of California Davis. February 2004.

10. Harvey, J., M. O. Bejarano, A. Fantoni, A. Heath, and H. C. Shin. *Performance of Caltrans Asphalt Concrete and Asphalt-Rubber Hot Mix Overlays at Moderate Temperatures – Accelerated Pavement Testing Evaluation.* Draft report submitted to California Department of Transportation. Pavement Research Center, CAL/APT Program, Institute of Transportation Studies, University of California, Berkeley. July 2000.

11. Harvey, J.T., J. Roesler, N.F. Coetzee, and C.L. Monismith. *Caltrans Accelerated Pavement Test (CAL/APT) Program Summary Report Six-Year Period 1994-2000.* Report prepared for the California Department of Transportation. Pavement Research Center, Institute of Transportation Studies, University of California Berkeley. June 2000.